THE EFFECTS OF THIN POLYMERIC SURFACE FILMS ON FRETTING CORROSION

by

Karl A. Sweitzer

Thesis submitted to the Graduate Faculty of the Virginia Polytechnic Institute and State University in partial fulfillment of the requirements for the degree of

MASTER OF SCIENCE

in

Mechanical Engineering

Approved:

N. S. Eiss, Jr. Chairman

H. H. Mabie

C. E. Knight

September 1984

Blacksburg, Virginia

DEDICATION

This thesis is dedicated to Melissa Jane Gale, who encouraged me to attend graduate school while we were friends and inspired me to finish this thesis while we were engaged.

ACKNOWLEDGMENTS

The author would like to express his sincere appreciation to the following people for their help in this research:

Dr. N. S. Eiss, Jr., his Major Professor, for his guidance and wealth of information.

Dr. H. H. Mabie and Dr. C. E. Knight for serving on his committee.

Shawn Daly, Janet Hein, and Ed Rhomberg, the student members of this research group for their thoughts and support throughout the first year of this project.

Mr. Maurice and Mrs. Alice Sweitzer, his parents, for their never ending support and encouragement.

The Army Research Office, for sponsoring this research.

TABLE OF CONTENTS

TABLE OF CONTENTS (Continued)

LIST OF FIGURES

LIST OF FIGURES (continued)

LIST OF TABLES

1.0 INTRODUCTION

Fretting corrosion has been studied extensively for the past thirty years. Most of the early work concentrated on fretting between unprotected metals. Now the research concentrates on ways to prevent fretting corrosion.

Past frettting corrosion experiments have showen that fretting between uncoated iron surfaces progresses in stages. Most investigators accept the concept of an initiation stage and a final steady state stage (although the wear mechanisms involved during these stages are widely debated). Methods for preventing fretting corrosion were similar to those used to prevent wear during sliding. Liquid and solid lubricants have been used in the fretting interface to reduce the shear stress between the contacting materials. Hardened contacting surfaces have also been used to reduce the real area of contact and to protect against abrasive wear.

Recent work at VPI&SU for the Naval Research Center has concentrated on reducing fretting at a bearing-cartridge interface. Initial work found that the relative motion between the bearing and cartridge is very complex and that its frequency is in a range from 15 Hz to 10 kHz. Grease, and solid lubricants in suspension, were found to reduce fretting corrosion in the interface.

This research considers the effects of thin polymer surface films on fretting corrosion. This research combines the experience obtained on fretting in a bearing-cartridge interface with the polymer wear experience accumulated at VPI&SU since 1973. New specimen holders for the bearing-cartridge fretting machine were designed to accept ball and

plate specimens. This new geometry approximates point contact sliding and is assumed to be less complex and more easily controlled. Additional instrumentation was added to the apparatus to measure the fretting friction force and electrical contact between the ball and plate. Four polymer films, two plate hardnesses and three plate surface topographies were tested for their fretting corrosion significance. Therefore, the main theme of this research was to:

1) Retard the start of the initiation stage by using polymer films to prevent metallic contact.
2) Determine if the polymer film on the ball could fret the metal plate, without metal–metal contact.
3) Study the protective qualities of different polymers.
4) Study how different metallic surface characteristics affect the thin polymer film's ability to protect the surface.

2.0 LITERATURE REVIEW

Fretting is a complex tribological phenomena that can arise when there is relative low amplitude motion between contacting surfaces. A very broad range of materials exhibit wear due to fretting. Fretting corrosion is most commonly associated with the build-up of oxide (αFe_2O_3) debris in steel interfaces. Fretting, as discussed in this thesis, will concentrate mainly on steel-steel and steel-polymer interfaces.

2.1 History and Reviews

Red iron oxide build-up at contacting interfaces was first reported by Eden, Rose and Cunningham [1]. Tomlinson [2], in 1927 was the first to investigate the problem and he described the mechanism as fretting corrosion. Tomlinson believed that the mechanism was one of "molecular attrition" where asperities were removed from the surfaces because of cohesion and then oxidized. In the 1950's, fretting was studied by many British investigators. New mechanisms were proposed and opinions about the effects of chemical and mechanical factors conflicted. Investigation continued through the 1960's and early 1970's when new scanning electron microscope (SEM) and x-ray photoelectron spectrometer (XPS) techniques were used to more accurately analyze the data. The delamination theory of wear developed by Suh [3] was later applied to fretting by Waterhouse [4] and Sproles and Duquette [5] in 1977.

In 1970, Hurricks [6] reviewed the existing mechanisms of fretting and summarized the sequence of events considered to occur as 1) the initial stage, 2) the debris generation state, and 3) the steady-

state. The initial stage is characterized by destruction of the existing oxide-metal surface layer, followed by adhesion and metal transfer. During the debris generation stage, wear debris is produced by mechanical-chemical action and forms a layer of reaction products that acts to produce metallic contact. A steady state production of debris then follows, where fatigue action rather than abrasion predominates.

Later, Waterhouse [7] gave a complete paper on all aspects of fretting. He concluded that:

> "Fretting corrosion can arise in any situation in which repeated relative movement occurs between contacting surfaces. The form and extent of damage depends on the chemical nature of the environment and on whether or not the debris can escape. On metals the debris is oxide with possibly some metal content. As initially produced, it has a plate like form and seems to arise from a process of delamination, either by the coalescence of subsurface voids or the propagation of fatigue cracks parallel to the surface."

Fretting and fretting corrosion have caused problems in a wide range of actual situations [7]. In machinery, fretting can occur between assemblies with small clearances such as taper fits, shrink fits, splines, couplings, keyways, and bearings. The relative motion can be caused by a dynamic source or from the vibration of a "rigid" fixture. Fretting can occur in screwed, bolted and riveted joints between the fastener and the joined pieces. If the fretting debris can escape from the interface, the joint will become loose. The loose debris itself can be hazardous. In orthopedic surgery, fractured bones are sometimes mended with metallic bone plates and screws. These joints sometimes fret and the debris can be very toxic. Aluminum oxide debris

is much harder than the parent metal and can act as an abrasive.

2.2 Wear Mechanisms

There is no fretting wear mechanism that all investigators accept. Most do agree though that fretting progresses in stages, and that fretting is influenced by a large number of variables. Therefore, no one theory can be accepted as correct with the exclusion of the others. With this understanding, the various electro-chemical and structural-mechanical factors that influence fretting will be discussed, with mention of the specific mechanisms that each investigator suggests. Then surface failure theories will be presented.

2.3 Mechanical Factors

The following mechanical variables may effect fretting: 1) sliding amplitude, 2) sliding frequency, 3) applied load, 4) surface topography, and 5) surface hardness.

2.3.1 Sliding Amplitude

Fretting implies relative motion but the limits of its range of amplitude are debated. Waterhouse [7] stated that fretting occurred within the amplitude range of 2-20 μm. Ohmae and Tsukizoe [8] studied the effect of slip amplitude over a range from 33-600 μm. Stowers and Rabinowicz [9] reviewed previous experiments with slip amplitude ranges from 10-300 μm and conducted their own from 12-400 μm. In 1939 Tomlinson, Thorpe, and Gough [10] reported fretting at as small an amplitude as 0.1 μm.

Ohmae and Tsukizoe, using a "specially designed detector" to

measure relative slip, found that...

> "At a constant number of cycles, fretting wear volume is dependent upon the slip amplitude and at constant sliding distance, the wear volume is small at slip amplitudes less than 70 μm. A rapid rise of wear volume is observed at larger slip amplitudes, and the wear volume approaches an almost constant value at much larger slip amplitudes (over 300 μm)."

Using x-ray microdiffraction techniques, and 100,000 cycle samples, they observed a change in the wear mechanism between small and larger slip amplitudes. At small amplitudes...

> "The surface region suffers from mild deformation and...the deeper part of the specimen is unaffected by the deformation. However, at larger slip amplitudes than 70 μm ...the extent of deformation is severe."

Waterhouse [7] states ...

> "There is general agreement that at amplitudes greater than 70-100 μm, the volume of material removed in a given number of cycles is directly proportional to the amplitude of slip."

Stowers and Rabinowicz [9] agree, but do not put this lower limit on the proportionality. They suggest that possibly ...

> "with decreasing amplitude ... the measured deflection is absorbed not into the surface asperities, but into the bulk of the testing machine between the interface and the point where the amplitude is finally measured."

2.3.2 Sliding Frequency

The sliding frequency seems only to effect the amount of time between cycles that a periodically exposed contact asperity is uncovered. When oxidation reactions are considered, Waterhouse [7] feels that frequency effects become negligible above 17 Hz. Stowers and Rabinowicz [9] after running experiments at 150-200 Hz adapt the Archard mild wear equation (1) to fretting

$$k = 0.3\ PV/LX \qquad (1)$$

where P = indentation hardness of the softer material

V = volume of material lost

L = normal load

X = total sliding distance, which in the fretting case is equal to 2aN, where a = peak to peak amplitude and N = number of cycles.

2.3.3 Normal Load

Although there is some disagreement, most curves of wear volume versus normal load are approximately linear. Increasing load has also been shown to decrease slip amplitude, thereby decreasing the total sliding distance and wear volume [7,9].

2.3.4 Surface Topography

Surface roughness is a parameter that is often omitted when fretting samples are described. When it is described, most experiments use polished surfaces. Suh [3] includes topography constants k_1+k_2 in the delamination equations, but does not describe them further.

2.3.5 Surface Hardness

Some experimenters consider material hardness to be a very important wear parameter. It is a factor in the Archard equation used by Stowers and Rabinowicz [9]. Early discussions of wear [11] use hardness values to calculate the real area of contact. Other experimenters do not feel that hardness is as important. Suh [3] does not directly include hardness in the delamination theory equations, and

Kayaba and Iwabuchi [12] after running experiments with five different upper and lower specimen hardnesses conclude that ...

> 1)"Hardness has only a minor influence on fretting wear. The significant factor is the action of the black oxide... and
> 2) in the absence of black oxide [αFe_2O_3], wear is directly dependent on hardness.
> 3) in some cases the wear of the hard specimen is greater than that of the soft specimen owing to the production of black oxide on the soft specimen."

2.4 Electrical and Chemical Factors

The environments in which fretting samples are tested can be described by their electrical, chemical, and thermodynamic properties. The chemical composition of the sample is also important. These factors will be discussed next.

2.4.1 Gaseous Environments

The chemical composition of gaseous environments can have a great influence on fretting. Unfortunately, experiments run in non-oxidizing atmospheres (nitrogen, helium, and hydrogen) give conflicting results. For example, Bethune and Waterhouse [13] found that fretting wear rates in nitrogen increased due to adhesion, but Feng and Uhlig [14] observed less wear in nitrogen than in air. [16] Kayaba and Iwabuchi [15] and Bill [16] performed much more rigorous experiments that showed that oxygen in the fretting environment has profound effects such as on the wear process. They found that surface oxide layers that grow on metals in high temperature applications can either reduce or increase fretting wear. Some metallic oxides act like solid lubricants while others act like abrasives. When the experiments were run without oxygen, the

metallic oxides did not form. The humidity of the environment is also a factor; fretting is usually reported to be less in more humid situations.

2.4.2 Liquid Environments

Experiments conducted with aluminum, copper, chromium, and other metal alloys in electrolyte media [7,18,19] show that friction and fretting can accelerate the destruction of protective surface films. Friction process can also facilitate their reformation. Waterhouse [7] states that ...

> "Disruption of the (surface) film by fretting can produce large changes in electrode potential, particularly on the baser metals such as aluminum and titanium. With aluminum in sodium chloride... the potential-time trace shows a rapid fall in potential as fretting commences, followed by fluctuating behavior characteristic of rapidly changing points of disruption and regrowth of the oxide film.

Waterhouse also found that fretting fatigue corrosion reactions can be controlled by impressing a cathodic potential on the electrolyte or a anodic potential on the metal. Although the results were based on fatigue life increases, a visual inspection of the surface showed much less damage. Clearly more investigation is warranted.

2.4.3 Thermal Environments

Fretting wear has been shown to decrease with increasing temperatures. The most accepted theory is that as the temperature increases, so does the thickness of the surface-oxide film. The oxide film becomes more adherent and acts like a solid lubricant, [7,16,17].

Studies [20] at room temperature have shown that the temperature in a fretting interface can be up to $20^{o}K$ higher than ambient, but not as

high as those increases measured for unidirectional sliding.

2.4.4 Specimen Elemental Composition

Adding small amounts of alloying elements to steels and other metals can increase the formation rate of protective surface oxide layers, [7,16]. Additional aluminum in nickel alloys has proved more successful than additional chromium especially at higher temperatures. In some stainless steel alloys, the increasing temperatures seems to favor a more abrasive chromium spinel instead of the protective chromium oxide Cr_2O_3, [7]. Subsurface voids and impurities are seen as sites where cracks form leading to delamination [3].

2.5 Polymer Fretting

Recent papers by Higham, Bethume, and Stott [21,22] have discussed the effects of experimental variables on fretting between polymers and steel. They have shown that some polymers can fret a 0.18 percent C, 0.73 percent Mn, 0.23 percent Si, 0.17 percent Ni, 0.23 percent Cr steel. Their major findings are summarized here (but discussed further in sections 6.1 and 6.5) for different polymers ...

> "1) the amount of wear of the steel increases in the order PTFE, LDPE, PVDF, PCTFE, PSF, PVC, PMMA, polycarbonate, Nylon 66.
>
> 2) there is a close correlation between the amount of metal wear and the surface energetics (in terms of the critical surface tension and coefficient of friction) of the polymer." [22]

For polycarbonate with various experimental conditions ...

> "1) It has been shown that polycarbonate can cause fretting damage to the steel surface during sliding in laboratory air, the damage involving transfer of $\alpha\ Fe_2O_3$ to the polymer surface.

2) The plots of wear against number of cycles shows three stages of damage: (a) an incubation period during which no wear of the steel takes place, (b) a running-in period during which the rate of wear decreases with number of cycles, and (c) a steady state period during which the rate of wear is fairly constant.

3) The air-formed film originally present protects the steel during the incubation period, but this film eventually breaks down and wear of the steel commences.

4) In general the amount of wear after a given number of cycles increases with increasing amplitude of slip, with decreasing frequency of vibration and with decreasing applied load.

5) The presence of water vapor is a necessary requirement for wear of the metal surface. The amounts of wear in moist O_2, moist A_2 and moist N_2 are greater than that in laboratory air, where very little wear occurs in dry O_2, dry A_2 or dry N_2." [21]

Unfortunately, very little else has been written (in English) about fretting polymers on metals.

2.6 Frictional Behavior of Polymer Films

During the 1970's, Briscoe et.al [23-27], studied the shear strength of thin polymer films under static and dynamic loading. They established a general linear equation [2] for the shear stress τ, for the static load case.

$$\tau = \tau_o + \alpha P \qquad (2)$$

where

τ = shear strength
P = contact pressure
τ_o and α = polymeric constants

Values for τ_o and α appear [24,25] for a range of polymers (and solvent-heat treatment variations). The viscoelastic nature of polymers suggest

a different mechanism for dynamic loading. The authors suggest equation (3), [27]

$$\tau = \tau_o' \, \ell n\left(\frac{V}{h\theta}\right) + \alpha P_o \exp\left(\frac{-V}{d\phi}\right) \tag{3}$$

where

V = sliding velocity

h = film thickness

d = contact length

P_o = applied load

θ, ϕ = relaxation frequencies

τ_o', α = polymeric constants

Although values for the constants and relaxation frequencies are not given, the authors state that further studies are underway. In the future then, Eq. (3) may be useful for studying fretting.

Other recent work by Ohara [28] suggest a new way of observing polymeric molecular changes during thin film friction. Measuring the thermally stimulated depolarization current (TSDC) can give information about changes in both the surface layer and the interior of the film. TSDC is described further in the Literature [28]. For instance, PVC tested at room temperature (22^oC) showed a build up of negative charges in the surface-layer produced by frictional electrification. Tests at elevated temperatures (73^oC) above the glass transition (72^oC) suggest that molecular segments or polar groups ($-C\ell$) are oriented during friction. The author suggests that this same re-orientation could also occur locally under higher loads.

Work has also been done to determine the properties of films transferred from a polymer slider to a metal disk under atomically clean conditions and large vacuums ($1x10^{-9}$ Torr), [29]. Using in situ Auger analysis, Pepper observed that PTFE transfers a PTFE film (several layers thick) to the sputter cleaned monel disk. PVC though, transferred a monolayer of chemisorbed chlorine on the nickel alloy surface. PTCFE transferred a monolayer also, but one with a composition closer to PCTFE. Pepper [29] feels that stick-slip sliding velocities and high shear stresses at the interface could initiate a decomposition or degradation chain scission removal of chlorine from PVC.

3.0 EXPERIMENTAL WORK

Table 1 is a listing of the experimental parameters used for this fretting corrosion research. These parameters and the rest of the experimental details will now be discussed further.

3.1 Test Specimens

The fretting experiments were run using AISI 1045 steel plates and AISI 52100 steel balls. The plates were turned to .975 in. (24.8 mm) dia. and .3125 in. (7.9 mm) thickness, and the balls are .625 in. (15.9 mm) dia.

Two plate hardnesses were investigated. The first was as received at 22.6 ± .5 Rockwell C (R_c). The second hardness was obtained by placing the plates in a furnace at 775° C for one hour, followed by a quench in ice water. The second hardness was 59.6 ± .9 R_c.

Two plate surfaces were also investigated. The first was achieved by surface grinding the hardened and unhardened plates. The average surface roughness perpendicular to the grinding marks was .368 ± .02 μm R_a. The second surface finish was achieved by wet sanding and polishing the ground surfaces. The sanding stages used 240, 320, 400, and 600 grit silicon carbide papers, followed by a final 1 μm aluminum oxide particle polish. The resulting surface finish had an average roughness .077 ± .01 μm R_a.

Before the balls were coated with polymer films, their surfaces were roughened, facilitating a good metal-polymer bond. Two procedures were used. The first was an electro-chemical etch using 10 percent (w/w) oxalic acid in distilled H_2O for 30-45 min using a 10V

TABLE 1

EXPERIMENTIAL PARAMETERS.

GEOMETRY	BALL ON PLATE (POINT CONTACT SLIDING)
LOAD	45 N (10 lbf)
AMPLITUDE	0.33 mm (0.013 in)
FREQUENCY	20 Hz
POLYMER FILMS	PTFE, LDPE, PVC, and PSF
BALL MATERIAL	AISI 52100 steel
PLATE MATERIAL	AISI 1045 steel
GROUND PLATE ROUGHNESS	0.368 ± 0.02 μm Ra.
POLISHED PLATE ROUGHNESS	0.077 ± 0.01 μm Ra.
STOCK PLATE HARDNESS	22.6 ± 0.5 Rockwell C
HARDENED PLATE HARDNESS	59.6 ± 0.9 Rockwell C
TEMPERATURE	21° C (70° F)
HUMIDITY	70%
ATMOSPHERE	NORMAL

potential. The second procedure was to sandblast the ball uniformly for about 3 minutes.

3.2 Polymer Films

Four polymer films were used to coat the balls: LDPE (low density polyethylene), PVC (polyvinylchloride), PSF (polysulfone), and PTFE (Teflon(polytetrafluroethylene)). The first three polymers were applied by solution casting. The balls were repeatedly dipped into 5 w/w solutions of polymer and solvent. The solvents used were chloroform for PVC, Tetrahydrofuran for PSF, and cyclohexane and paraxylene for LDPE. The LDPE solutions had to be heated to 50^{o} C, which reduced the solution viscosity, allowing thin film formation. After each dip the films were allowed to air dry for one minute. Then after the final dip, the balls were placed in a vacuum dessicator for 48 hours to remove the remaining solvents.

The PTFE film was built up by repeatedly dipping the balls into a dispersion of Teflon and water. After each dip, the balls were placed in an oven at 380^{o} C to cure the deposited film. The curing time was determined visually by the transition of the Teflon film from its original white-opaque state to its cured translucent state. After the transition, the balls were removed from the oven and allowed to cool to room temperature before the next dip.

3.3 Ball on Plate Tribometer

The Mark III B is a modified version of the existing Mark III machine which was used for previous fretting corrosion experiments. The

Mark IIIB has three main parts:

1. A vibration fatigue testing machine,
2. A drive linkage that converts the vertical motion of the vibration testing machine to lower amplitude horizontal motion, and
3. Specimen holders that secure the ball and plate, but more importantly, give strain and electrical contact data that can be monitored during the experiment.

The original Mark III was designed so that the deflection of the apparatus would be much less than the fretting amplitude when the total horizontal friction force was 1500 N. Complete dimensions and displacement calculations for the Mark III are given elsewhere [30]. For our experiments the total horizontal friction force was assumed to be less than 130 N. Therefore, the apparatus deflections are minimal.

Figure 1 is a drawing of the Mark IIIB. The three main parts of the Mark IIIB will now be discussed further.

3.3.1 Fatigue Testing Machine

The Fatigue Testing Machine is the source of the relative motion needed when studying fretting corrosion. The All American Vibration Fatigue Testing Machine, model #10-VA-T, built by the All American Tool & Manufacturing Company of Skokie, IL, consists of four components: a variable speed drive motor, a vertical motion shaker table, a motor speed control, and a frequency readout gage. The variable speed motor drives an eccentric in the vibration machine which displaces the shaker table vertically. The table's displacement is adjusted by varying the eccentricity, and its frequency is adjusted by the motor speed

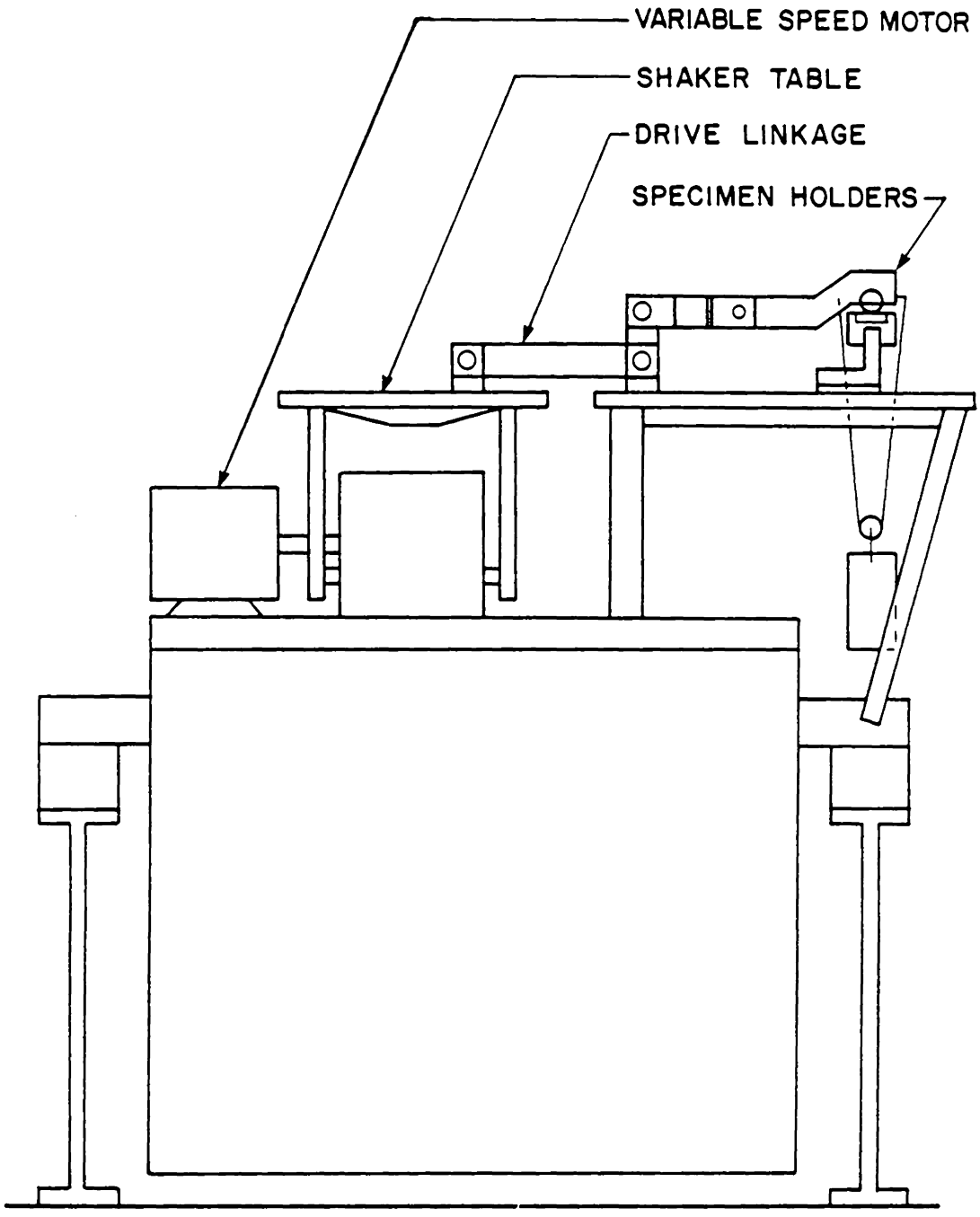

FIGURE 1. MARK III B FRETTING MACHINE

control. The whole Mark IIIB is mounted on a concrete block, and isolated from the floor by four vibration isolation mounts.

3.3.2 Drive Linkage

The drive linkage was designed to convert the vertical motion of the shaker table to 5X lower amplitude horizontal motion needed for fretting corrosion experimentation. Figure 2 is a drawing of one side of the symmetric drive linkage. The heart of the linkage is the motion conversion arms. The pivot points of the motion conversion arms are attached to the stationary base plate by base plate mounting blocks. The motion conversion arms are attached to the shaker table and to the drive bar by shaker table and drive bar mounting blocks, respectively. The motion conversion arms are attached to three shafts that attach to bearings that are housed in the mounting blocks. Each mounting block has two bearings which straddle the motion conversion arms.

3.3.3 Specimen Holders

For the current experiments, new specimen holders were designed by the author to secure the balls and plates. The Mark III B has two positions where experiments can be run simultaneously. Figure 3 shows how the two holders function together. The more complex holder is for the ball, which will be discussed first.

Each ball is connected to the drive bar of the Mark III B via a ball strain arm. This arm was designed with two thin sections where strain gages are mounted so that the frictional force between the ball and the plate can be monitored during the experiments. Figure 4 shows an isometric view of the ball strain arm. The vertical centers of the

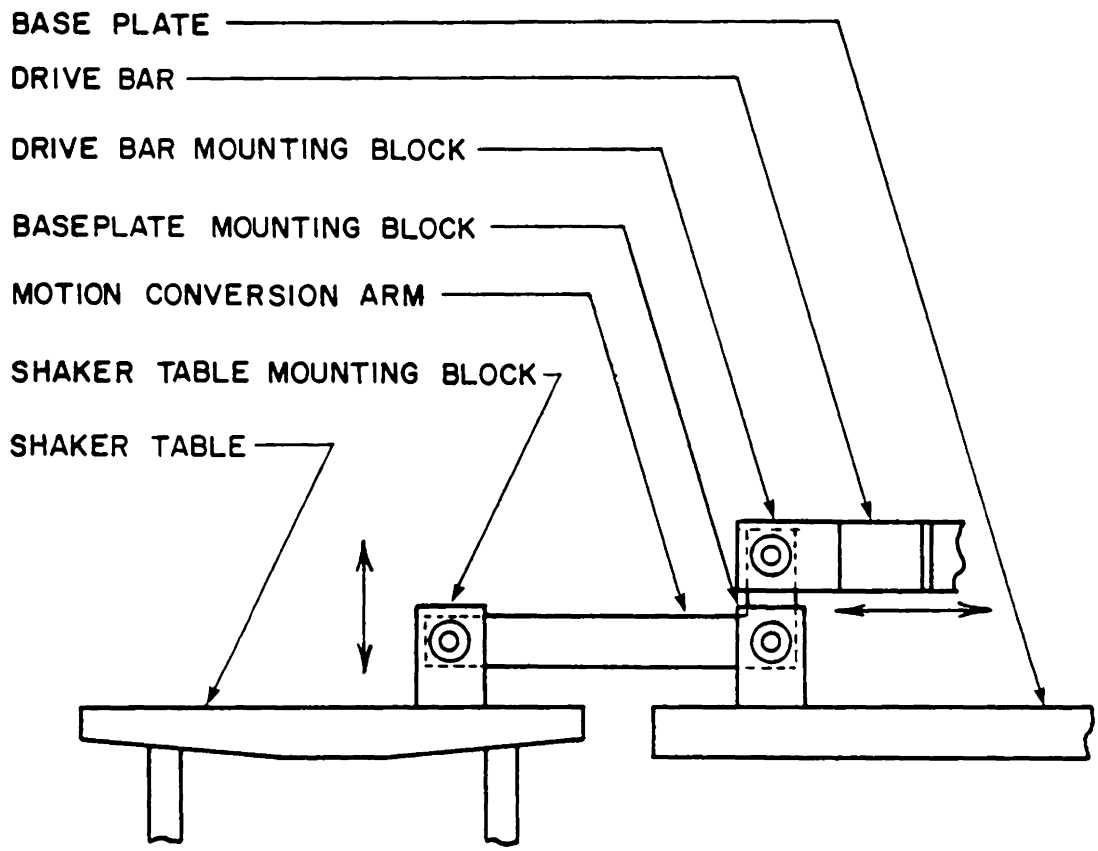

FIGURE 2. DRIVE LINKAGE

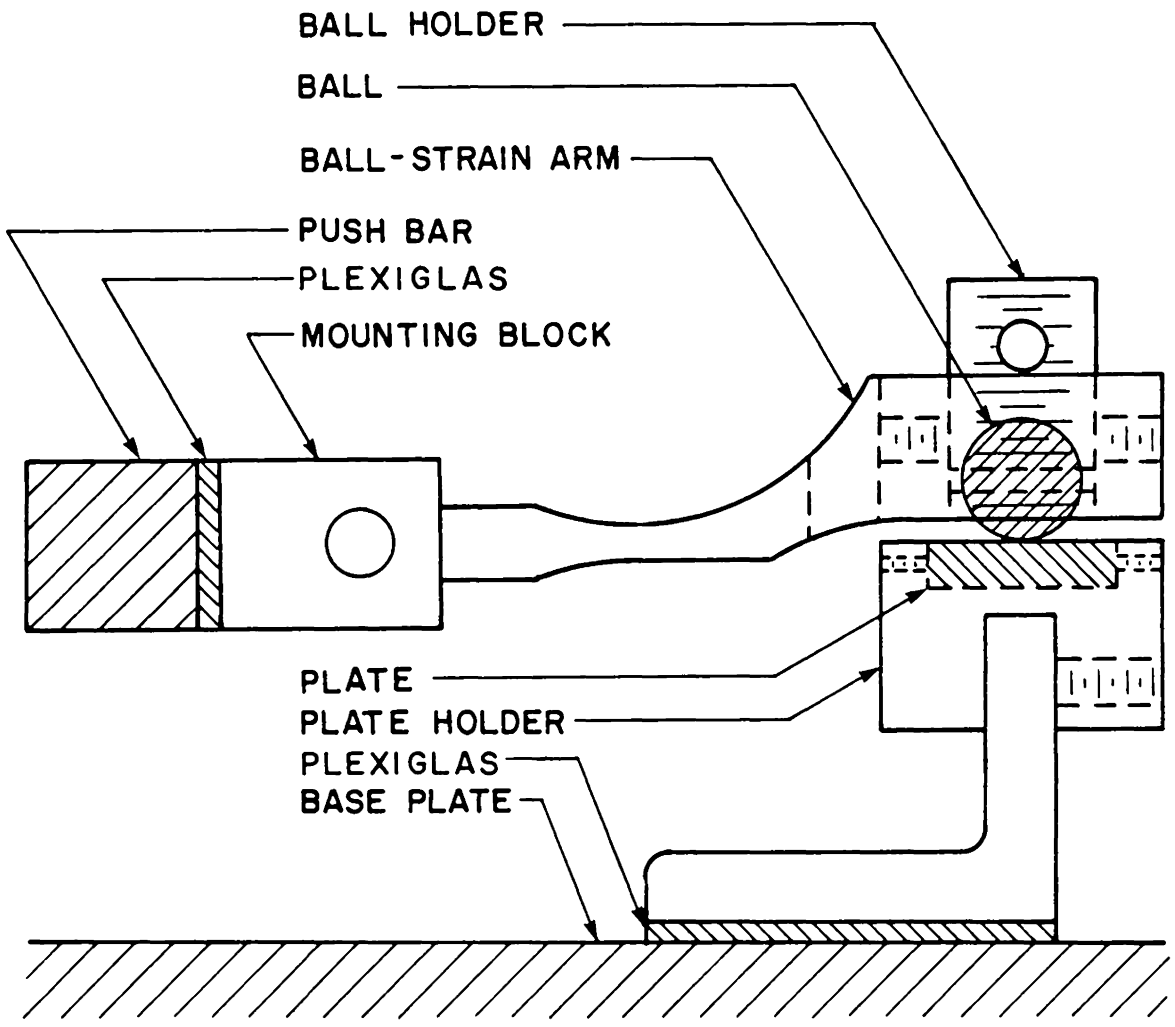

FIGURE 3. BALL AND PLATE SPECIMEN HOLDERS

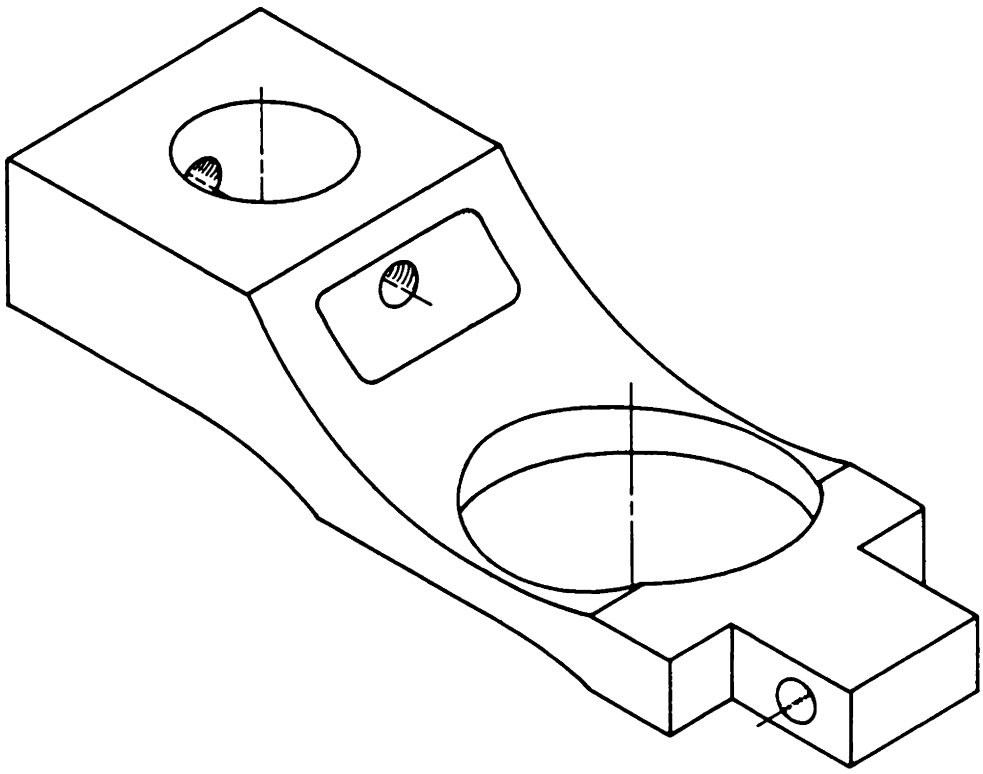

FIGURE 4. BALL-STRAIN ARM

thin sections are in line with the point of contact between the ball and the plate. This eliminates bending moments on the thin sections and results in only axial forces (and displacements). A 2-element 90^{o} rosette strain gage is mounted on the inside face of both thin sections forming a full bridge poision-configuration strain gage circuit. The strain gage leads are connected to a Vishay/Ellis -11 amplifier whose output is then monitored by a Gould 220 2-Channel strip chart recorder. Each of the two apparatus positions has its own amplifier and strip chart recorder.

The ball-strain arm and its instrumentation were calibrated in two steps. First, known weights were hung along the centerline of the thin-sections of the ball-strain arm. This corresponds to the pull stroke of each cycle. Then, the instrumentation was corrected for dynamic response errors. Figure 5 is a comparison of strip charts from the friction force trace for experiment PSF HA 13-1 and a 20 Hz square wave signal from a wavetek Model 110 function generator. The solid bands were drawn when the chart speed was 1 mm/sec and the harmonic waves were drawn when the chart speed was 125 mm/sec. The width of the solid bands correspond to a true value term plus a recorder response term. Least squares linear regression equations were fitted to the static weight and the recorder response error data. These equations were then combined so that the absolute value of the friction force could be found knowing the width of the band drawn for the friction force.

The ball is held in the ball strain arm by two cylindrical ball holders that contact the ball at two latitudinal circles $\pm 33^{o}$ from the equator of the ball. The bottom holder is fixed in the ball strain arm

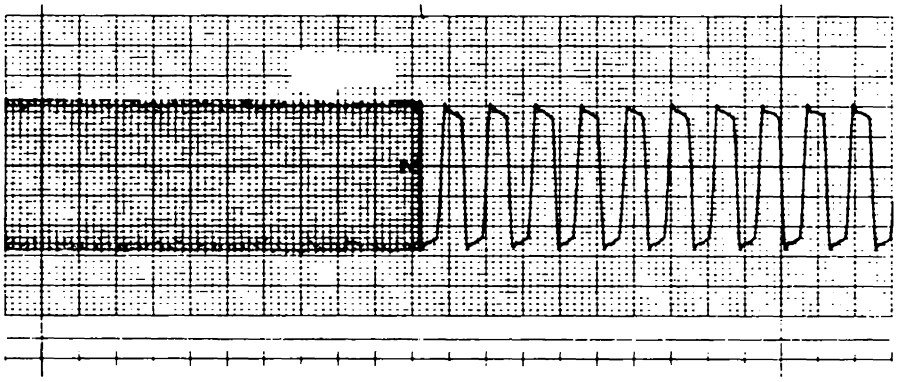

CHART SPEED: 1 mm/sec 125 mm/sec

FRICTION FORCE TRACE FOR PSF EXPERIMENT HA13-1.

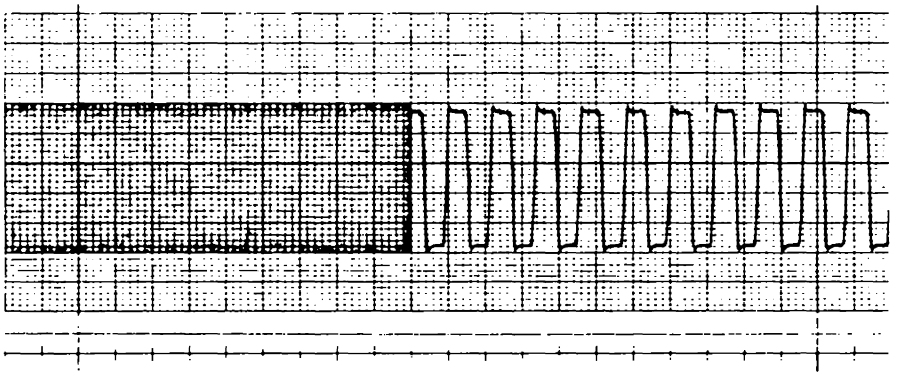

CHART SPEED: 1 mm/sec 125 mm/sec

20 Hz SQUARE WAVE SIGNAL RESPONSE.

FIGURE 5. STRIP CHART DATA COMPARISON.

and allows the ball to protude ≈ 1/8" (3.2 mm) below the surface of the holder. The top holder has 3/4-16 UNF threads that allow it to be drawn down tightly against the ball, thereby fixing the ball in the ball strain arm.

Two load bolts intersect the top holder on its center line. These are then tightened down on the top holder locking it in place. Load wires hook over the bolts and shot filled canasters are suspended from the wires.

The ball strain arm is attached to the Mark III B drive bar by a mounting block. This block has two BG-36 Torrington extra precision needle bearings that support the shaft from the ball strain arm, and allow it to move vertically. The mounting block and the drive bar are separated by a 1/8" (3.2 mm) thick piece of Plexiglas (PMMA) which acts as an electric insulator between the two metal pieces when they are bolted together with two 10-24 UNC nylon bolts.

The plate holder is the second of the two specimen holders. It has a hole in its center that accepts the 1045 steel plate specimens. The plate is then held in place by two set screws. The plate holder also has a channel machined in it that allows the plate holder to be placed over, and positioned along a section of angle iron. The plate holder is held in position on the angle iron by two set screws. The angle iron is then attached to the base plate by bolts. Once again, the angle iron and the aluminum base plate are separated on a 1/8" (3.2 mm) thick piece of Plexiglas (PMMA). The 6 steel bolts are isolated from the angle iron by plastic bushings and Plexiglas (PMMA) washers.

Each apparatus position is now electrically connected by a common

ground, the angle iron, and isolated from the rest of the Mark III B. The two ball strain arms, and the angle iron are also connected to an electrical/circuit that is designed to place a 15 mV potential across the ball and plate polymer interface. When the polymer film in the contact zone breaks down, and metal asperities from the ball touch the asperities from the plate, the electrical potential across the interface goes to zero, and a short circuit registers on the strip chart recorder. Figure 6 is a diagram of this electrical (metal-to-metal) contact monitoring circuit.

3.4 Mounting Specimens and Running Experiments

There are four main steps needed to start up and run the ball and plate experiments:

1) mount plate and its holder,
2) secure ball in ball-strain arm,
3) apply loads, and
4) activate monitoring instrumentation and fatigue machine.

These four steps will now be discussed in detail.

3.4.1 Mount Plate and Its Holder

The plate specimen is first secured in the plate holder. When ground plates are used, the grinding marks are aligned either parallel or perpendicular to the sliding direction. Set screws in the plate holder are tighten down on the plate, holding it in position. Next the plate holder is placed on the angle bracket and positioned under the ball hole in the ball-strain arm. A second set of set screws in the

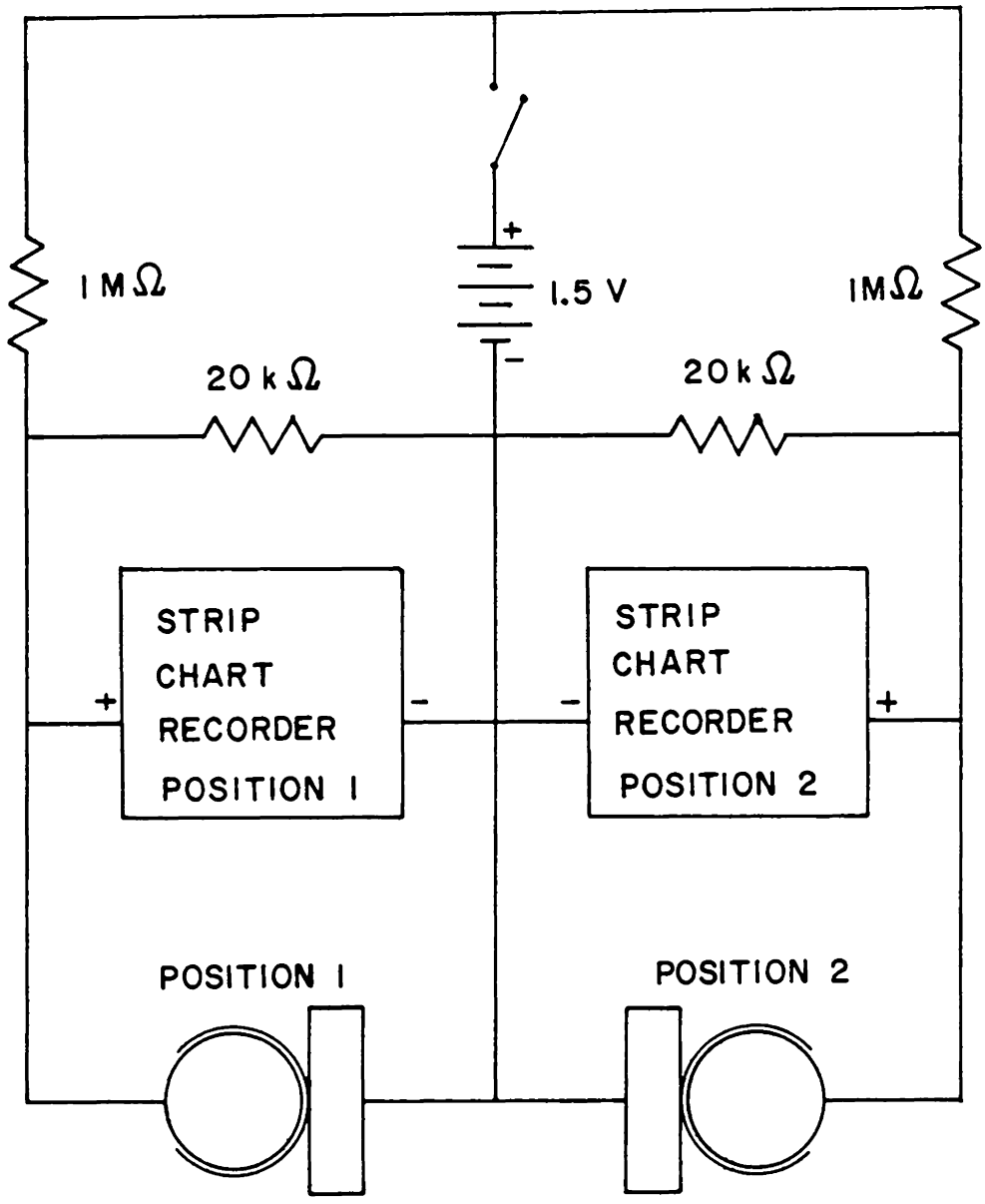

FIGURE 6. ELECTRICAL CONTACT MONITORING CIRCUIT

plate holder fixes its position on the angle bracket.

3.4.2 Secure ball in Ball-Strain Arm

The ball is placed into the strain arm with the aid of a suction hose. One end of the hose has a suction circle that has the same curvature as the ball. When the ball is placed in the suction circle, with a fresh polymer film area up, the experimenter sucks on the other end of the hose, holding the ball in position. The ball can then be lowered into the ball holder in the ball-strain arm. The upper ball holder is then tightened down on the ball, with the aid of a metal rod placed through the two holes in the holder. The two load bolts are then tightened down on the upper ball holder.

3.4.3 Apply Loads

The rear load bolt has the load wire attached to it permanently via a washer/hook. The other end of the load wire attaches to the front load bolt via a hook eye. With the load pulley placed over the center of the load wire, the wire is fed up through the base plate and hooked over the front load bolt. The load canister is then hooked into the eye of the load pulley. Before continuing, the load wires must be positioned along the load bolts so that the wires do not touch the plate holders or the base plates.

3.4.4 Activate Monitoring Instrumentation and Fatigue Machine

The motor speed controller must first be turned on so that it can warm up before starting the experiment. The strip chart recorders, the

strain gage amplifiers and the electrical contact circuit are then switched on. Then the strip chart is set into motion by selecting the desired rate (usually 5 mm/sec). The strain gage signal is then centered in its scale by adjusting the balance on the amplifier, and the electrical contact signal is checked to assure that it has not grounded out on the apparatus. Finally, the stop watch is started while the speed controller is adjusted to give the desired frequency (usually 20 Hz). After 60 sec. the chart rate was usually reduced to 1 mm/sec.

When the experimenter decides to stop the experiment, the steps are repeated in reverse order.

4.0 RESULTS

Like the original Mark III, the Mark III B could produce fretting samples after a short period of time. For this fretting corrosion study, it was decided to only run the experiments until the polymer film broke down in the contact region. If fretting wear debris was produced, no attempt was made to quantify the amount of damage.

4.1 Shake Down Tests

Once the modifications to the Mark III were completed, shakedown tests were run to check the instrumentation and the ball on plate fretting behavior. The Mark III B performed well in these tests, but the monitoring instrumentation had to be developed further. The electrical contact system was changed twice before reaching its final configuration. Early attempts using an oscilloscope to monitor the contact signals were plagued by ambient electrical interference. Strip chart recorders proved less prone to electrical interference but more apt to mechanical vibration interference. The two strip chart recorders had to be placed on a separate table, away from the strain gage amplifiers. Electric fans in the recorders emitted 60 Hz noise that was picked up by the strain gage amplifiers. The recorders also had to be placed on 3/4" (19 mm) foam rubber to further isolate them from the instrumentation.

The early fretting experiments also showed us that the polymer films could indeed help lengthened the time before the start of corrosion. Uncoated balls were tested and found to give obvious fretting debris after only 600 cycles. The ball coating procedures were perfected and samples were prepared for the remaining experiments.

4.2 Data Analysis

The effects of the experimental parameters were analyzed by three techniques: 1) photographic, 2) electrical contact, and 3) frictional force. Each has its advantages and will be discussed next.

4.2.1 Photographic Data

A WILD mm 420 macroscope, equipped with the WILD MPS 55/51 Photo Automat and Shutter piece connected to a Leitz 35 mm film carrier was used to photograph the results of these experiments. 200 ASA Kodak Ektachrome color slide film was used for most of the photographs. The macroscope and camera were calibrated so that both quantitative and qualitative measurements of the fretting damage could be recorded. The magnification of the image on the 35 mm slide ranged from 5.04:1 at the lowest zoom setting of 6.3 to 25.60:1 at the highest 32 setting. Two sources of quartz halogen light were used: coaxial incident illumination, directed along the viewing path, and side illumination using two flexible fiber optic light wands. The fiber optic light wands are attached to a VOLPI Intralux 6000 quartz halogen light source. The coaxial illuminator has built-in polarizing filters whose degree of extinction can be varied with a rotatable quarterwave plate. Rotating the quarterwave plate changes the contrast effects that are desirable when photographing polymer-coated samples.

The photographic data proved most valuable for the calculation of the polymer film thickness at the point of contact. Photographs of the balls after they had been worn in the fretting apparatus were enlarged and measurements were taken of the projected images. Examples of these

photographs are shown in Figures 7 and 8. Knowing the ball radius r_o, and the image factor I, the film thickness h can be found by measuring the diameter of the polymer contact area D_1 and the metal contact area D_2. The derivation of Eq. (4) can be found in Appendix C.

$$h = \sqrt{r_o^2 + \left(\frac{D_1^2 - D_2^2}{4I^2}\right)} - r_o \qquad (4)$$

where

h = film thickness

r_o = ball radius

D_1, D_2 = measured contact diameters from projected ball images

I = image factor depending on original zoom magnification

Equation 4 assumes that the worn area on the ball is a plane. Figure 7 shows a ball just after it had full electrical contact. Notice the small central area that is assumed to be the contacting surface of the metal ball. The diameter of this area is D_2. Fig. 8 shows a ball from an experiment where there was large amounts of fretting oxide debris formed but no electrical contact. The author assumes that the outer ring (D_1) in this figure is the polymer film region, and the central area corresponds to the worn area of the ball (produced by abrasive wear, discussed in Section 5.2.2). If the polymer film and ball wear areas do not form a plane then the calculated film thicknesses will be incorrect.

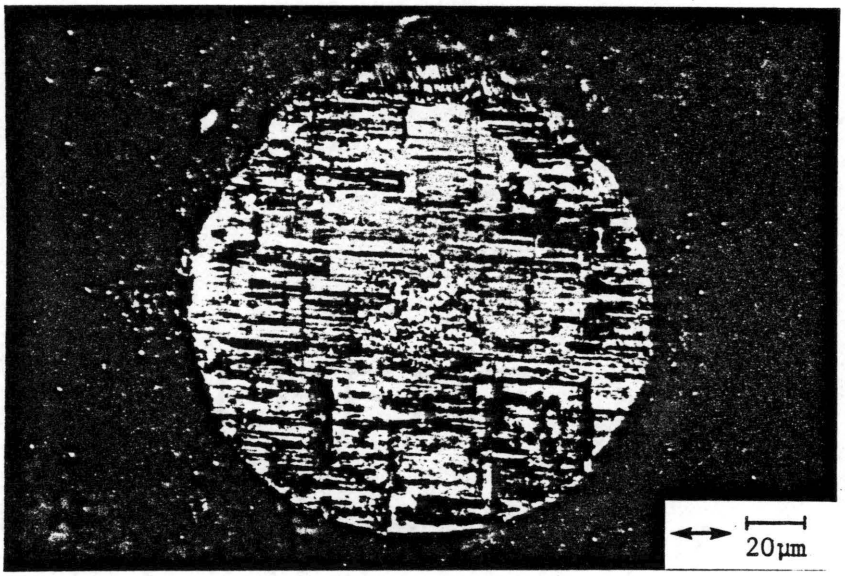

Figure 7. PVC ball #36 with hardened plate #17-1, after sliding against lay for 108 seconds.

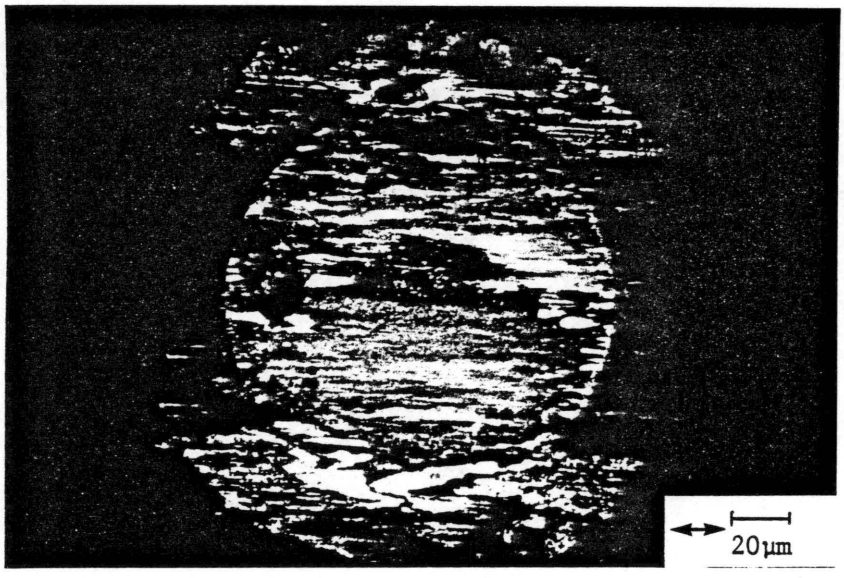

Figure 8. LDPE ball #26 with hardened polished plate #02-5, after sliding for 2870 seconds.

4.2.2 Electrical Contact

Monitoring electrical contact was originally suggested so that we could determine when metal-to-metal contact occurred between the ball and the plate. The transitions from polymer film protraction (no electrical contact) to polymer film failure (full electrical contact) were divided into five catagories dependent on the length and type of transition. They are: 1) Abrupt, 2) Gradual, 3) Intermittent, 4) Grouped, and 5) Mixed, and 6) No Contact.

The Type 1 transitions started before the 400 cycles and occurred over less than 40 cycles. Type 2 transitions are similar to Type 1 but they start after 20 to 36,000 cycles and last for up to 800 cycles. Other types of transitions are characterized by periods of contact during longer periods of no contact. Type 3 transitions have sudden one or two cycle contact periods before the start of the transition to full contact. Type 4 transitions have intermittent contact periods that can last over a thousand cycles before the final transition period to full contact. Type 5 transitions are characterized by transition periods to full contact followed by further transitions back and forth between contact and no contact. They lasted from 8000 to 16,000 cycles but could have lasted longer had the experiment not been stopped during transition.

Some experiments never had electrical contact. These are Type 6 transitions. The longest no-contact run was 80 minutes.

4.2.3 Frictional Force

Once the friction force instrumentation was calibrated, the frictional force could be determined by measuring the width of the force band and substituting that into the calibration equation. During the experiments, the frictional force would change. After the first few transient cycles (typically 20 cycles), the friction force would reach an initial value that would change further depending on what was happening in the interface. The minimum (after the transient phase) and maximum frictional forces were calculated and used to statistically analyze the effects of the three parameters. The maximum friction force showed no statistical significance but the minimum did. The analysis of variance tables generated using this friction force data are given in Appendix B.

4.3 Experiments

Three parameters were varied during the experiments: 1) polymer film type, 2) plate hardness, and 3) surface topography. Time till electrical contact and frictional force were the variables measured during the experiments. The data from the experiments is assembled in Appendix A.

4.3.1 Polymer Film Type

The most significant parameter in these experiments was the polymer film composition. Each polymer gave significantly different mean minimum friction forces and different electrical contact characteristics. Table 2 gives a listing of these for each polymer, and

TABLE 2

MEAN MINIMUM FRICTION FORCES AND DISTRIBUTION OF ELECTRICAL CONTACT TRANSITION TYPES BY POLYMER.

Polymer	Mean Minimum Friction Force (Normal load = 45 N)	Transition Type 1	2	3	4	5	6
PTFE	4.4 N	2 13%	2 13%	2 13%	0 0%	6 41%	3 20%
LDPE	9.3 N	8 40%	4 20%	2 10%	2 10%	0 0%	4 20%
PVC	16.2 N	0 0%	8 42%	4 21%	3 16%	1 5%	3 16%
PSF	24.5 N	0 0%	2 16%	2 16%	1 8%	3 23%	5 37%

Figure 9 shows the mean friction forces and their standard deviations for each polymer film type. Notice that each polymer has a different predominant transition type and that it is about 40 percent of the total. Appendix A has the data grouped by the particular ball used for each experiment, and includes a column for the number of times each ball was dipped into the polymer coating solution. Appendix C gives the film thickness data calculated using photographic techniques. The electrical contact data for each polymer will now be discussed further.

The time until initial contact (I.C.) column in Appendix A shows that PVC films gave a wide range of I.C. times. Table 2 shows that the predominant transition for PVC was the gradual Type 2. The shear strength of PVC is higher than LDPE and PTFE, and this could explain why its electrical contact transition is gradual. The PVC film may gradually break down in a brittle manner, and then not be able to repair itself.

LDPE and PVC films gave similar results. The chemical composition of their polymer chains are identical except that one of every four hydrogens in the PE chain is replaced by a chlorine to form PVC. LDPE had the most Type 1 transitions and all of the Type 2 transistions occurred before about 2000 cycles. If there was to be electrical contact, the initial contact occurred before about 2000 cycles. The shear strength of LDPE films is much less than PVC which may explain why the LDPE films wore through quickly.

PSF films gave the most no contact runs and the highest friction forces. PSF also gave a range of times to initial contact. It was the only polymer film that could last in the interface when fretted

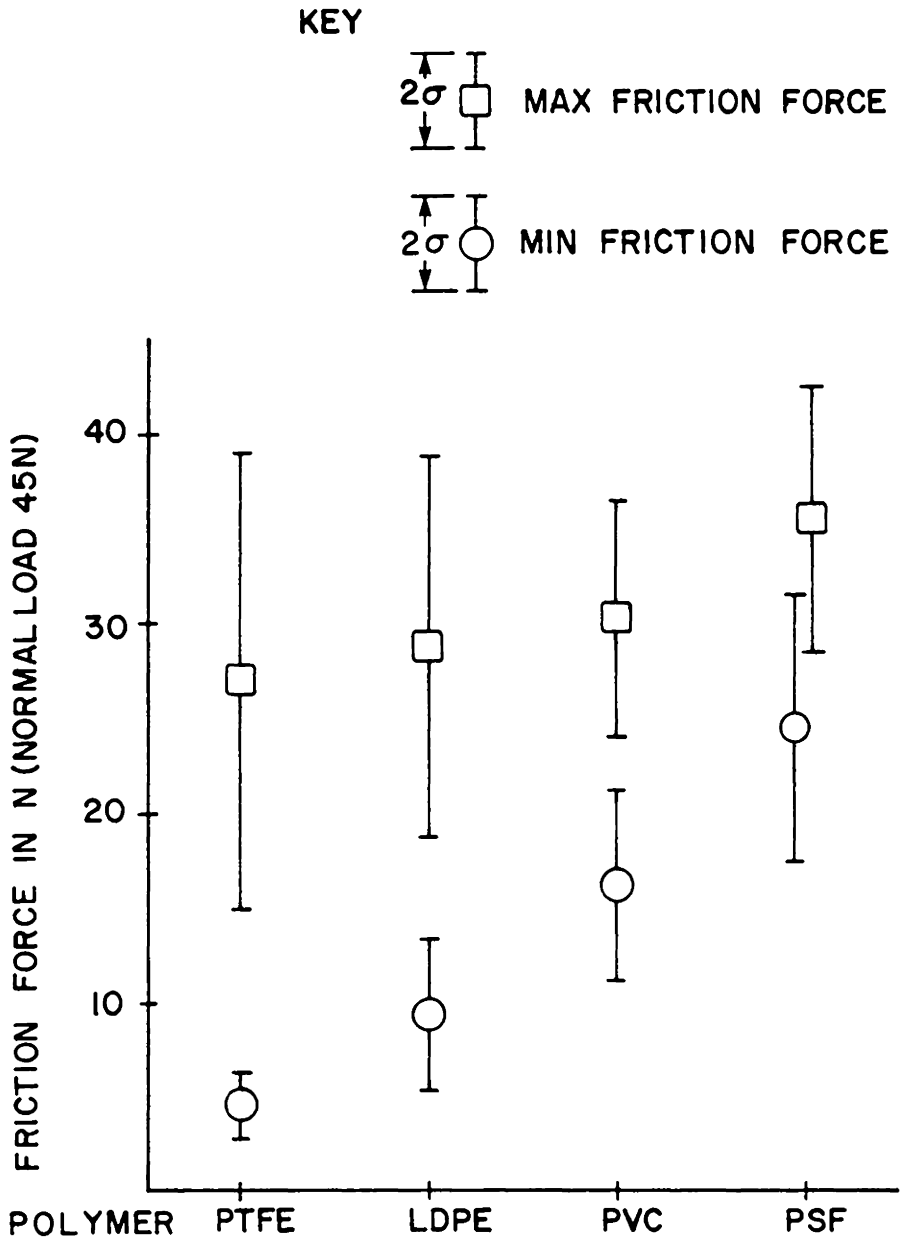

FIGURE 9. MEAN MAXIMUM AND MINIMUM FRICTION FORCE VS POLYMER FILM TYPE

perpendicular to the surface grinding marks.

PTFE films gave the lowest friction forces and more Type 5 transistions than all of the other experiments combined. Molecular PTFE is also similar to Polyethylene except that all the LDPE hydrogen atoms are replaced by flourine atoms. PTFE is known to transfer in layers during sliding and this could account for its apparent ability to repair itself during fretting.

4.3.2 Plate Hardness

Figure 10 shows that the mean minimum friction forces (within a polymer type) are not significantly different when plate hardness was the dependent variable. This data is given numerically in Appendix B Tables 2B-5B. A review of the electrical contact data does not show any differentiating trends either. There are four times as many Type 2 and 4 transitions with hardened plates but they are concentrated in the PVC results.

4.3.3 Surface Topography

Figure 11 shows that the mean minimum friction forces (within a polymer type) are not significantly different when surface finish was the dependent variable. This data is given numerically in Appendix B Tables 6B-9B. When the PSF experiments are not included, 80 percent of the no contact runs were against polished plates. When the PSF experiments are included, 87 percent of the no contact runs were against either polished plates or ground-parallel plates.

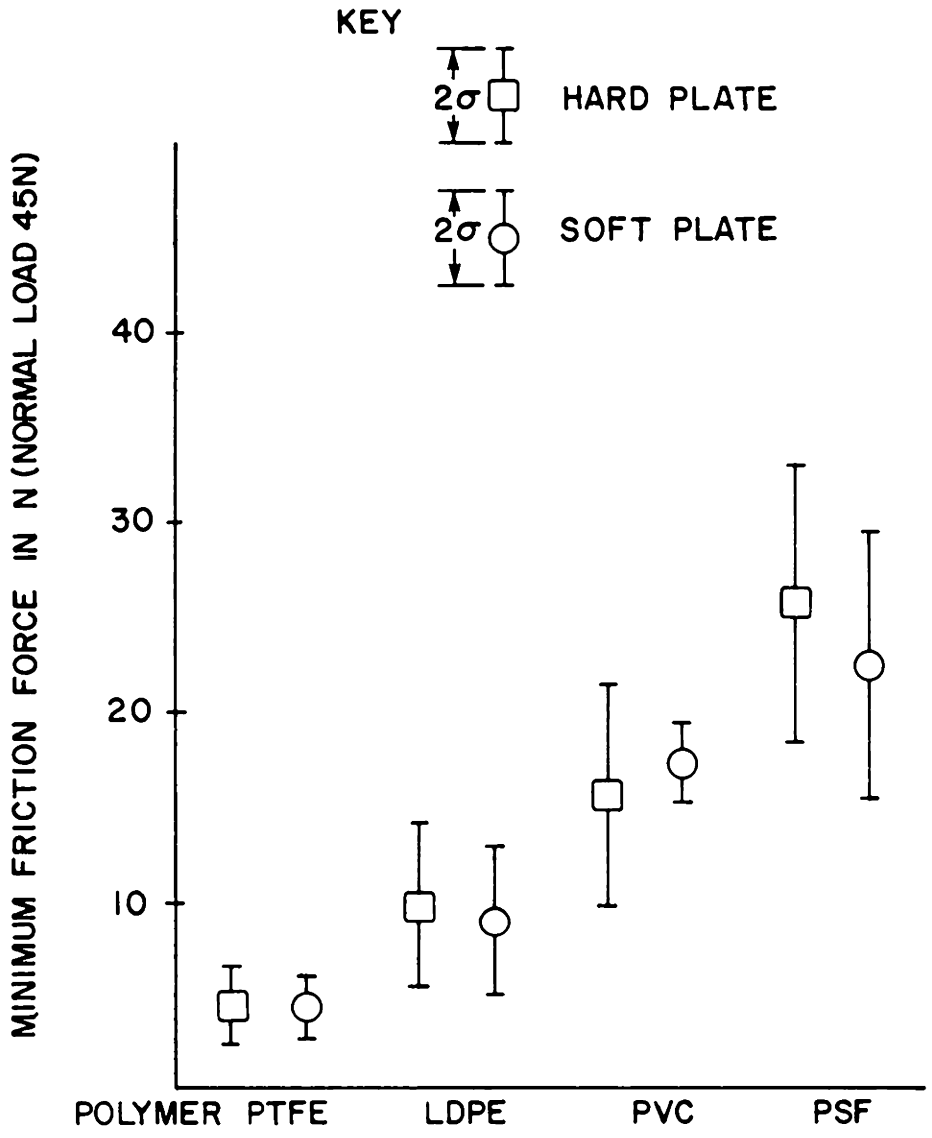

FIGURE 10. MEAN MINIMUM FRICTION FORCE VS PLATE HARDNESS AND POLYMER FILM TYPE

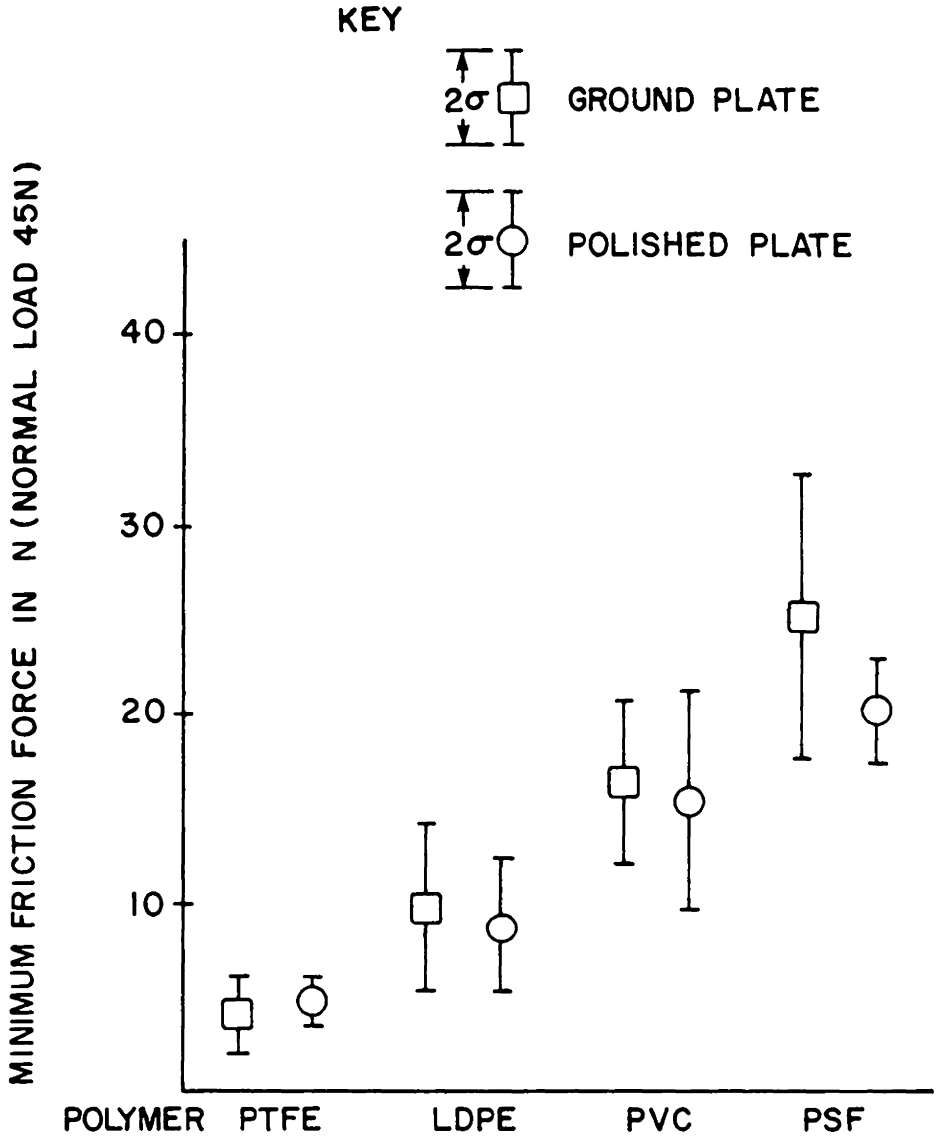

FIGURE 11. MEAN MINIMUM FRICTION FORCE VS PLATE SURFACE AND POLYMER FILM TYPE

5.0 DISCUSSION

The purpose of this research project was to study the effects of thin polymeric surface films on fretting corrosion. A ball on plate tribometer, with various thermoplastic ball coatings, was used. Metallic contact between the ball and plate was monitored during the experiment with an electrical contact circuit. The frictional force between the ball and the plate was also monitored.

5.1 General Findings

All of the polymers tested could prevent electrical contact for at least 40 minutes. PVC was the only polymer that could prevent metallic contact (after 60,000 cycle) and not fret the metal plate. Experiments run with ground plates oriented perpendicular to the sliding direction showed piles of polymer debris that had been worn from the ball's polymer coating (see Figures 12 and 13). This process usually took only 1000 cycles. Plate hardness didn't affect the results.

5.2 Fretting by Polymeric Films

PTFE, LDPE, and PSF films could prevent metal-metal contact for over 60,000 cycles, but they also fretted the steel plates. Figures 14 and 15 show hardened ground plates that were fretted by a PSF coated ball for 72,000 cycles without electrical contact. Notice how pits have formed at the edge of the polymer contact region. Also notice the transferred material layers throughout the polymer contact region. Figures 16 and 17 show hardened polished plates that were fretted by a LDPE coated ball (Figure 8) for 57,400 cycles without electrical

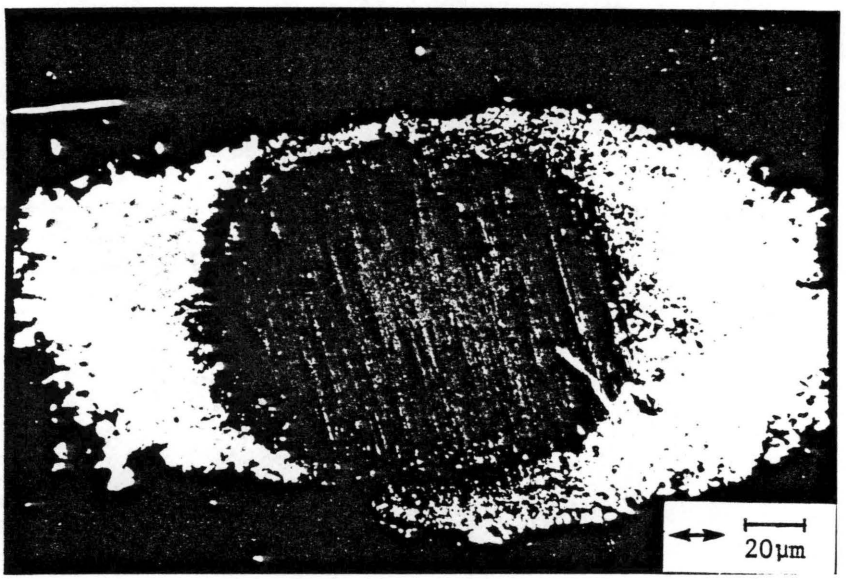

Figure 12. Hardened plate #04-2 with PSF ball #13, after sliding against lay for 77 seconds.

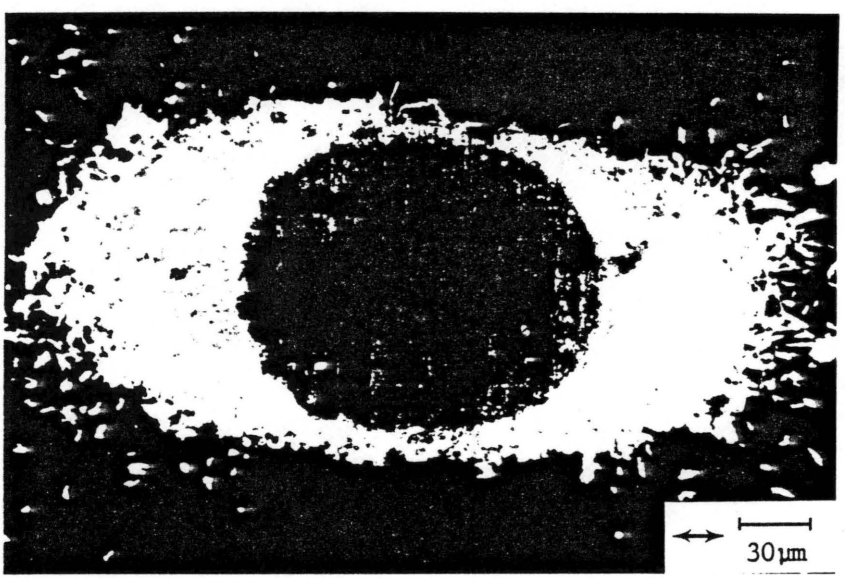

Figure 13. Hardened plate #17-1 with PVC ball #36, after sliding against lay for 108 seconds.

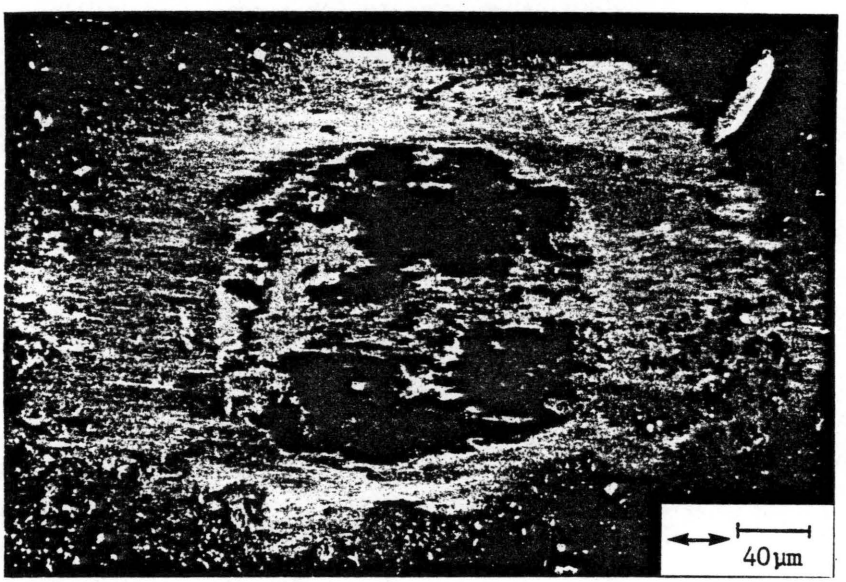

Figure 14. Hardened plate #13-2 with PSF ball #42, after sliding with lay for 3590 seconds.

Figure 15. Hardened plate #13-2 with PSF ball #42, after cleaning with acetone.

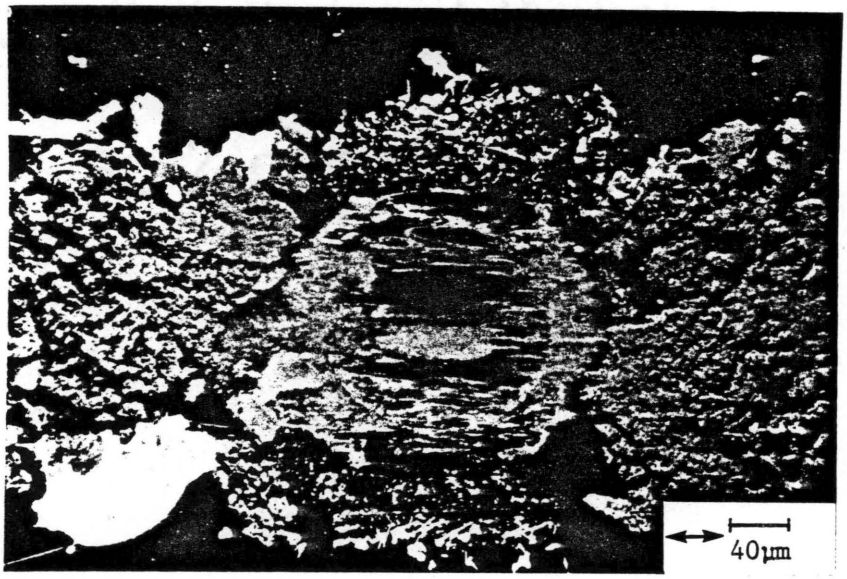

Figure 16. Hardened polished plate #02-5 with LDPE ball #26, after sliding for 2870 seconds.

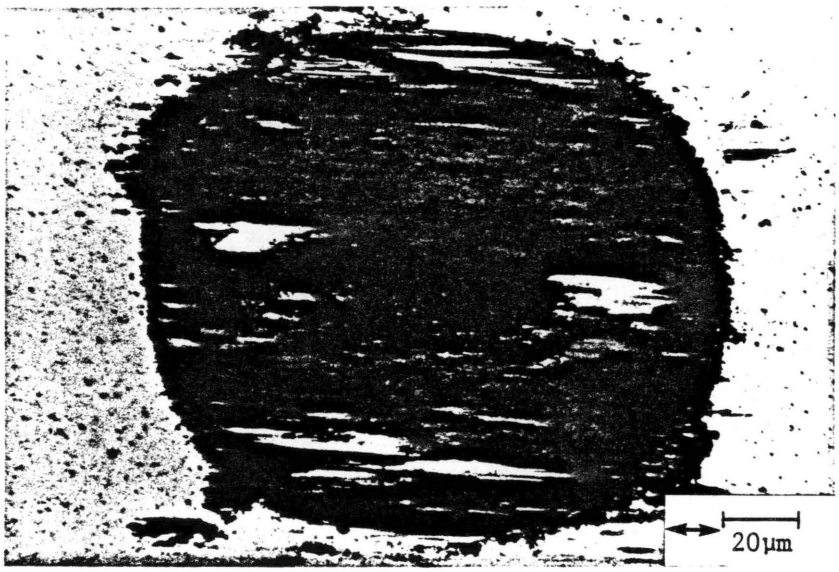

Figure 17. Hardened polished plate #02-5 with LDPE ball #26, after cleaning with acetone.

contact. The cleaned plate surface (Figure 17) shows evidence of pitting and the ball shows evidence of wear. Notice how the surface film seems to be a mixture of polymer and oxide. The color slide of Figure 8 shows that the film over the worn area is the same orange-red color as the oxide debris in Figure 16.

5.2.1 Fretting Mechanisms

In the initial stage of fretting in these experiments, oxidation seems to be the major mechanism but abrasion is also thought to occur. There are two oxidation reactions that can be suggested:

1) Uhlig's theory [6,14] where asperities scrape off oxide layers, exposing clean active metal which further reacts with the oxygen in the air forming oxide debris.
2) Oxidation-reduction where a change in oxygen potential in the contact region starts an electro-chemical corrosion reaction that continues in the fretting interface.

The first mechanism has been discussed in detail [6]. It is a viable mechanism and recent experiments at elevated temperatures suggest that if the oxide layer is formed in the interface, and not removed, then the oxide layer can act like a solid lubricant, preventing wear.

The second mechanism is an extension of the first, but concentrates more on electro-chemical oxidation-reduction reactions. It will now be discussed further.

5.2.2 Oxidation-Reduction in Fretting Interface

Before beginning this discussion, some assumptions about the surface layer on the steel plate have to be discussed. Figure 18 shows

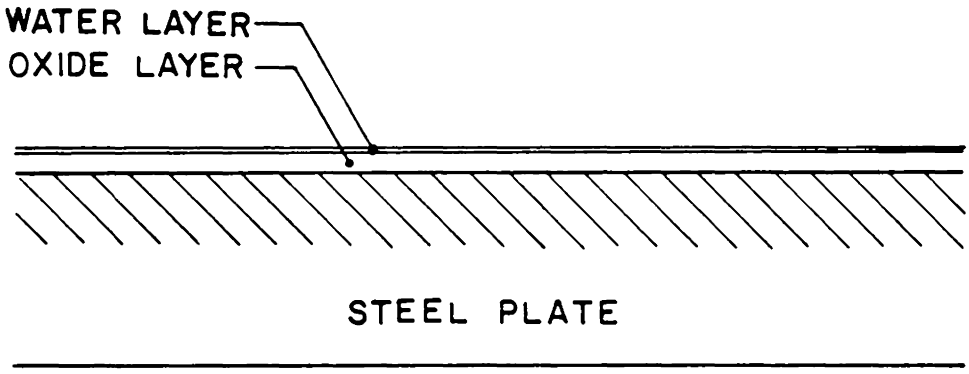

FIGURE 18. AMBIENT SURFACE LAYERS

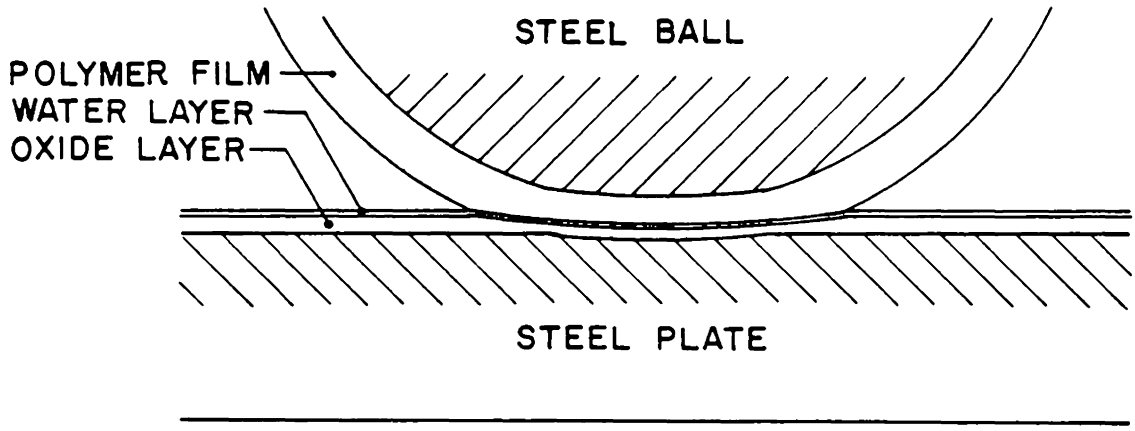

FIGURE 19. SURFACE LAYERS UNDER LOAD

the assumed layers. The steel surface is first covered by a chemisorbed oxide layer (and possibly other gases) with a molecular layer of water forming the second layer. This water layer is assumed to contain enough chlorine to make it electrolytic. Now, Figure 19 shows the assumed surface layers under loaded conditions.

After the experiment starts, it is thought that some of the oxide layer in the contact area begins to be removed. The contact area now has less oxygen than the rest of the plate. This oxygen difference starts a concentration cell that provides a potential to drive the electro-chemical corrosion reaction. The anode is the surface of the plate under the contact area. The iron gives up two electrons forming the anode half-cell reaction (5). The electrons then flow though the bulk of the steel plate to the perimeter of the contact area.

$$Fe \rightarrow Fe^{++} + 2\,e \qquad (5)$$

At the perimeter, which forms the cathode, the reaction is assumed to be oxygen reduction (6).

$$O_2 + 2H_2O + 4e \rightarrow 4OH^- \qquad (6)$$

The OH^- ions can then flow through the electrolytic monolayer and react with the iron in the contact area (7). The electrolytic monolayer completes the electrical corrosion circuit.

$$Fe^{++} + 2OH^{-} \rightarrow Fe(OH)_2 \qquad (7)$$

The motion of the ball then pushes the ferrous hydroxide to the ends of its stroke where it is further reacted with oxygen in the air (8).

$$4\ Fe(OH)_2 + 7O_2 \rightarrow 2\ Fe_2O_3 + 8H_2O \qquad (8)$$

The preceding development is analogous to the corrosion mechanism accepted for rust forming around the perimeter of a water droplet on steel, [31,32].

There seems to be considerable evidence for this fretting corrosion mechanism. The fretting experiments discussed earlier (Section 2.4.2) in electrolytic solutions [18], showed larger current flows once fretting was started. The polymer fretting experiments conducted in moist environments [21] showed that fretting wear increased in a humid environment. Figure 15 of our experiments show pits just inside the polymer contact perimeter. The oxide debris is then found in piles at the ends of the sliding stroke (Figure 14). Irregularities that occur in the polymer film interface could create additional paths for the electrolytic water layer, further continuing the corrosion process. Waterhouse [7] also showed that the fretting fatigue life of samples in an electrolite could be increased dramatically with an applied cathode voltage of 1200 mv.

5.2.3 Abrasion in Fretting Interface

Buildup of oxide debris in the contact interface is assumed to be

the start of a second wear mechanism. Microscopic investigation has shown that the interface polymer film can change to a darker brown color indicating mixing of polymer and oxide debris. This mixture, while still preventing electrical contact, could act an an abrasive. Figures 8, and 16 show a LDPE ball and plate that ran for 57,400 cycles with no metal contact. Figure 8 shows a set of circles corresponding to the edge of the polymer film and the interface between film and ball. These circles all seem to lie on a plane, indicating removal of a spherical segment of polymer film and steel.

This abrasive wear mechanism can be placed in the second stage of fretting corrosion. Initial oxide debris had to be formed before it could mix with the polymer to form the abrasive medium.

5.3 PVC Protection Mechanism

Now that a corrosion mechanism has been proposed, the following assumptions about the PVC protection are given. Studies by Pepper [29] showed that PVC transfers a monolayer of chlorine atoms to the surface of a metal during sliding in a vacuum. It is assumed that a similar event happens in our fretting experiments. Figures 20 and 21 show plates that were run with PVC coated balls. Notice that there is a film on the plate surface. If chlorine is indeed deposited onto the plate surface then it is assumed that the oxygen concentration cell is not created. Now that chlorine is in the interface, it is assumed that the charge differential between the contact area and the rest of the plate is much less. Therefore, the iron anode half-cell reaction is less likely to initiate.

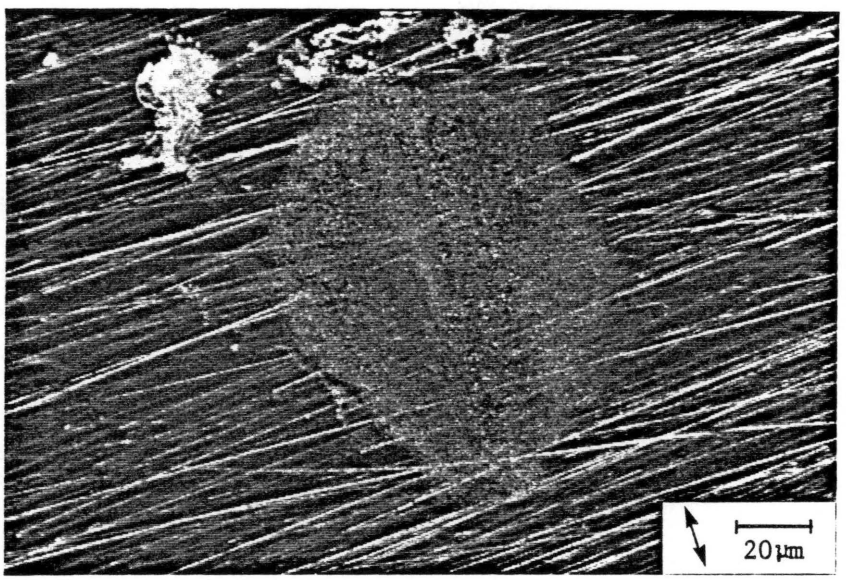

Figure 20. Hardened polished plate #10-2 with PVC ball #15, after sliding for 3009 seconds.

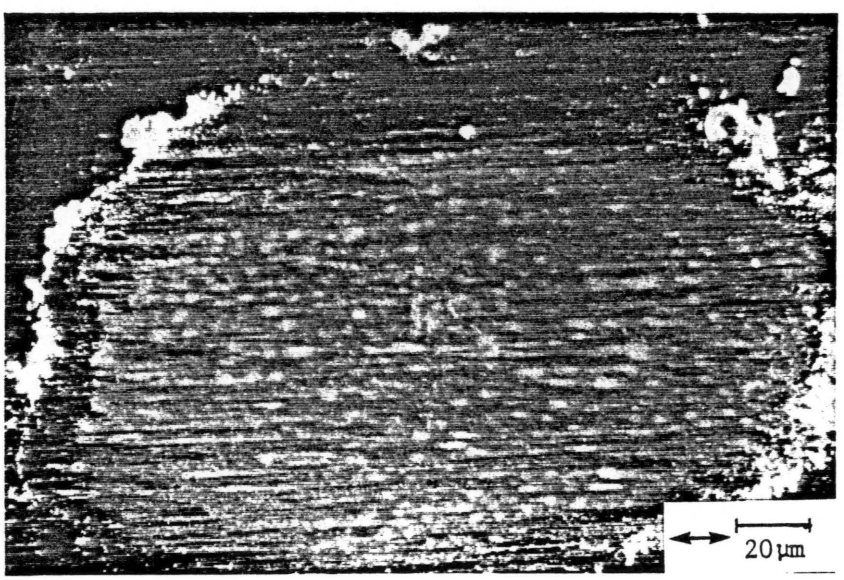

Figure 21. Ground plate #03-1 with PVC ball #5, after sliding with lay for 5600 seconds.

5.4 Friction Force in Fretting Interface

There was no statistical significance between the mean maximum frictional forces and polymer types. The maximum friction forces usually occurred after electrical contact so this implies that the maximum friction force was characteristic of metal-metal sliding. This was most dramatic for PTFE because its friction force was very low before contact. With PVC, the maximum was usually soon after electrical contact, but with LDPE, the force level tended to increase gradually after electrical contact. PSF would sometimes show a decrease in frictional force after electrical contact. The frictional force data was useful for comparing the effects of the different experimental parameters. The mean minimum frictional force showed significant differences when compared between polymer types. The shear strengths of the polymer films [24] are different and could explain the different friction forces.

5.5 Electrical Contact Transistions

Each of the polymers showed different predominant transition types. PVC and LDPE had the most short-gradual transitions, while PSF and PTFE had more grouped and intermittant transitions. Very few of the balls that had multiple runs gave the same transition type for each run. PVC, PSF, and PTFE all gave a range of times until initial contact, but LDPE had initial contact before about 2000 cycles. LDPE has a low shear strength which may explain its short time until initial contact. When LDPE had no contact it is assumed that oxide debris mixed with the polymer in the interface forming a stronger more abrasive

material. Initial contact times may be correlated with the initial surface oxide layer thickness. Further research may show this oxide layer correlation and therefore substantiate the electro-chemical corrosion mechanism.

6.0 CONCLUSIONS AND RECOMMENDATIONS

6.1 Conclusions

This research has helped the author reach the following conclusions:

1. The measured mean minimum friction forces are a function of polymer film type and increase in the order PTFE, LDPE, PVC, and PSF.
2. The distributions of transitions between polymer film protection and polymer film failure are different for each polymer film composition.
3. The initial fretting corrosion mechanism may be due to electro-chemical oxidation-reduction reactions that are driven by the formation of a oxygen concentration cell in the contact region.
4. Oxide debris formed by the initial electro-chemical corrosion mechanism may mix with polymer in the interface forming an abrasive medium. This abrasive medium then helps sustain fretting corrosion.
5. PVC films may protect against fretting corrosion. Chlorine atoms from the PVC molecular chain may transfer to the plate thereby reducing the electrical concentration potential cell in the contact region. The proposed electro-chemical corrosion mechanism needs the concentration cell to drive the oxidation-reduction reactions.

6.2 Recommendations

Further questions about fretting corrosion have been generated during this research and further investigation is recommended. Modifying the apparatus will allow us to control more of the experimental conditions and to record additional data. Additional experiments could help test different fretting situations and substantiate proposed theories. Additional analytic work could also help us derive formulas for predicting the extent of protection or distruction.

6.2.1 Apparatus Modification

Surface oxide and water layers are assumed to play a very important role in the fretting corrosion process. Studies in a sealed chamber could allow us to control the amount and composition of the environment surrounding the experimental samples. More instrumentation could also allow us to monitor additional parameters during the experiment. Monitoring the displacement at the fretting interface would eliminate errors due to deflection of the strain gage force transducers, and could give more information about the time history of the sliding process. Measuring the current flow through the samples could help substantiate the proposed electro-chemical corrosion process. Knowing the change in temperature in the interface could help us understand how the polymer film behaves during the initial fretting stages.

6.2.2 Further Tests

This research has shown that polymer films can help prolong the start of fretting corrosion. Running new tests with controlled environments could help us understand what role the oxide and water layers play in the fretting corrosion process. Additional tests with other metals and polymers would also expand our knowledge of useful fretting combinations.

The electro-chemical fretting corrosion mechanism suggested in this thesis should be substantiated by running tests in controlled atmospheres. One of the main assumptions was that the water in the air could form an electrolytic molecular layer on the surface of the metal plate. This theory could be tested by controlling the humidity and the concentration of electrolyte in the atmosphere around the fretting samples. Tests with non-oxidizing gases would also eliminate the possibility of the oxygen reduction cathode reaction (6).

Tests with other metals that form surface oxides could also test this theory. Aluminum and stainless steel alloys are good candidates that also have common and practical applications.

PVC seems to give good results under our conditions so other halogenated polymers might give similar results. Sequentially substituting halogens for hydrogen on the polyethylene chain could test the effects of polarity and element type. Other polymer film application methods might also give more reproduceable and homogeneous films. Sputter coating techniques are currently being investigated. Different ball surface preparations could also be evaluated for their effectiveness.

Finally, cathodic-anodic potentials have been shown to increase fretting fatigue life in electrolytic solutions [7]. Applying similar potentials to our experimental samples could further test the proposed electro-chemical corrosion mechanism.

6.2.3 Additional Data Analysis

Along with testing new parameters should come ways of quantifying their effects. Additional methods for examining the physical and chemical changes should also be explored.

The scanning electron microscope (SEM) should be used more often to get a magnified look at the fretted surfaces and oxide debris. Chemical changes at the surfaces should also be studied using auger electron spectroscopy and x-ray and electron diffraction techniques. Knowing the surface oxide layer thickness would be a first step in quantifying its protective qualities. X-ray diffraction has also been used successfully for determining the chemical composition and structure of oxide debris.

Thermally stimulated depolarization currents [28] have been suggested as a technique for observing polymer molecular changes during friction, and could be adapted to our future studies. Further chemical analysis of the polymer debris and polymer-oxide mixtures is also recommended. Nondestructive techniques for measuring the polymer film thickness are also needed.

6.2.4 Additional Analytic Investigation

The electro-chemical fretting corrosion theory presented in this thesis should be studied further in terms of the corrosion kinetics and

currents involved. With additional analytic development the corrosion currents and potentials could be predicted. The buildup of protective oxide layers on the free surface of the metals should also be considered. Others have suggested a fracture mechanism approach [17] to the destruction of surface oxide layers in the fretting interface.

REFERENCES

1. Eden, E. M., Rose, W. N., and Cunningham, F. L., Proc., Inst. Mech. Eng., London, 4 (October 1911) 839. Cited by V. V. Kovalevskii, "The Mechanism of Fretting Fatigue in Metals," Wear, 67 (1981), pp. 271-285.

2. Tomlinson, G. A., "The Rusting of Steel Surfaces in Contact," Proceedings of the Royal Society, Ser. A, 115 (1927), pp. 472-486.

3. Suh, N. P., "The Delamination Theory of Wear," Wear, 25, (1973), pp. 111-124.

4. Waterhouse, R. B., "The Role of Adhesion and Delamination in the Fretting Wear of Metallic Materials," Wear, 45 (1977), pp. 355-364.

5. Sproles, E. S., Jr., and Duquette, J. D., "The Mechanism of Material Removal in Fretting," Wear, 49 (1978), pp. 339-352.

6. Hurricks, P. L., "The Mechanism of Fretting - A Review," Wear, 15 (1970), pp. 389-409.

7. Waterhouse, R. B., "Fretting," Treatise on Materials Science and Technology, 13 (1979, pp. 259-286.

8. Ohmae, N., and Tsukizoe, T., "The Effect of Slip Amplitude on Fretting," Wear, 27 (1974), pp. 281-294.

9. Stowers, I. F., and Rabinowicz, E., "The Mechanism of Fretting," Journal of Lubrication Technology, Trans. of ASME, 95 (1973), pp. 65-70.

10. Tomlinson, G. A., Thorpe, P. L., and Gough, H. J., "An Investigation of the Fretting Corrosion of Closely Fitting Surfaces," Proceedings, Institution of Mechanical Engineers, 141, #3 (1939), pp. 223-249.

11. Bowden, F. P., Moore, A. J. W., and Tabor, D., "The Ploughing and Adhesion of Sliding Metals," Journal of Applied Physics, 14 (1943), pp. 80-91.

12. Kayaba, T., and Iwabushi, A., "Effect of the Hardness of Hardened Steels, and the Action of Oxides on Fretting Wear," Wear, 66 (1981), pp. 27-41.

13. Bethune, B., and Waterhouse, R. B., "Adhesion of Metal Surfaces Under Fretting Conditions, I: Like Metals in Contact," Wear, 12 (1968), pp. 289-296.

14. Feng, I. M., and Uhlig, H. H., "Fretting Corrosion of Mild Steel in Air and in Nitrogen," Journal of Applied Mechanics, 21, 4 (1954), pp. 395-400.

15. Rhee, S. K. Ruff, A. W., and Ludema, K. C., Ed.,Wear of Materials, The American Society of Mechanical Engineers, New York (1981).

16. Bill, R. C., "The Role of Oxidation in the Fretting Wear Process," Ref. 15, pp. 238-250.

17. Kayaba, T., and Iwabuchi, A., "The Fretting Wear of 0.45 Percent Carbon Steel and Austentic Stainless Steel from 20°C up to 650°C in Air," Ref. 15, pp. 229-237.

18. Bethune, B., and Waterhouse, R. B., "Electrochemical Studies of Fretting Corrosion," Wear, 12 (1968), pp. 27-34.

19. Aronov, V. and Yahalom, J., "Studies on the Behavior of Copper During Friction Under Electrolyte Immersion Conditions," Wear, 47 (1978), pp. 293-299.

20. Sproles, E. S., Jr., and Duquette, D. J., "Interface Temperature Measurements in the Fretting of a Medium Carbon Steel," Wear, 47 (1978), pp. 387-396.

21. Higham, P. A., Bethune, B., and Stott, F. H., "The Influence of Experimental Coditions on the Wear of the Metal Surface During Fretting of Steel on Polycarbonate," Wear, 46 (1978), pp. 355-350.

22. Higham, P. A., Stott, F. H., and Bethune, B., "The Influence of Polymer Composition on the Wear of the Metal Surface During Fretting of Steel on Polymer," Wear, 47 (1978), pp. 71-80.

23. Briscoe, B. J., Scruton, B., and Willis, F. R., "The Shear Strength of Thin Lubricant Films," Proceedings of the Royal Society, London, A333(1973), pp. 99-114.

24. Amuzu, J. K. A., Briscoe, B. J., and Tabor, D., "Friction and Shear Strength of Polymers," American Society of Lubrication Engineers Transactions, 20(4) (1977), pp. 354-358.

25. Briscoe, B. J. and Smith, A. C., "The Influence of Solvent and Thermal History on the Friction of Polymeric Films," Friction and Traction, Ed. by Dowson, D., Taylor, C. M., Godet, M., and Berthe, D., Westbury House, Guildford, England, (1980), pp. 99-104.

26. Briscoe, B. J. and Smith, A. C., "The Influence of Dynamic Loading on Sliding Friction," Nature, 278 (1979), pp. 725-726.

27. Briscoe, B. J., and Smith, A. C., "The Effect of Periodic Loading on the Shear Strength Properties of Thin Organic Polymeric Films," American Society of Lubrication Engineers, Transactions, 23(3) (1980), pp. 232-236.

28. Ohara, K., "Molecular Processes During Friction of Polymer Films Observed by Thermally Stimulated Depolarization Currents," Wear, 73 (1981), pp. 147-155.

29. Pepper, S. V., "Auger Analysis of Films Formed on Metals in Sliding Contact with Halogenated Polymers," Journal of Applied Physics, 45 (1974), pp. 2947-2956.

30. Frantz, R. D., "An Experimental Study of Fretting Corrosion at a Bearing/Cartridge Interface," Masters Thesis, Virginia Polytechnic Institute and State University, February 1983.

31. Flinn, R. A. and Trojan, P. K., Engineering Materials and Their Applications, 2nd Edition, Houghton Mifflin Company, Boston, MA, pp. 505-507.

32. Masterton, W. L. and Slowinski, E. J., Chemical Principles, 4th Edition, W. B. Saunders Company, Philadelphia, PA, pp. 573-574.

33. Ott, L., An Introduction to Statistical Methods and Data Analysis, 2nd Edition, Duxbury Press, Boston, Mass., pp. 325-376.

APPENDIX A

RAW DATA FOR THIN POLYMER FILM RESEARCH.

NOMENCLATURE:

POLY.....POLYMER FILM TYPE
B#.....BALL NUMBER
#D.....NUMBER OF DIPS INTO POLYMER SOLUTION
PLATE.....PLATE CODE (MSNN-E) WHERE,
    M.....MATERIAL TYPE; H = HARDENED, A = AS RECEIVED
    S.....SURFACE TYPE; W = GROUND WITH, A = GROUND AGAINST,
          AND P = POLISHED
    NN.....PLATE NUMBER
    E.....EXPERIMENT NUMBER
TOTAL.....TOTAL RUN TIME (sec)
I.C.....TIME UNTIL INITIAL ELECTRICAL CONTACT (sec)
F.C.....TIME UNTIL FINAL ELECTRICAL CONTACT (sec)
T.....ELECTRICAL CONTACT TRANSISTION TYPE (6 = NO CONTACT)
MX.lb.....MAXIMUM FRICTION FORCE IN POUNDS
MX.N.....MAXIMUM FRICTION FORCE IN NEWTONS
MN.lb.....MINIMUM FRICTION FORCE IN POUNDS
MN.N.....MINIMUM FRICTION FORCE IN NEWTONS
NA.....DATA NOT AVAILABLE

				RUN TIME DATA				FRICTION FORCE DATA			
POLY	B#	#D	PLATE	TOTAL	I.C.	F.C.	T	MX.lb	MX.N	MN.lb	MN.N
PVC	14	5	HW13-3	1679	1609	1616	2	7.84	34.88	3.19	14.20
PVC	15	5	HP10-2	3009	NA	NA	6	NA			
PVC	15	5	HP10-3	211	NA	NA	6	5.05	22.47	4.12	18.34
PVC	15	5	HP10-4	2399	NA	NA	6	8.76	39.02	3.19	14.20
PVC	15	5	HW11-5	221	149	199	4	5.42	24.12	4.54	20.19
PVC	15	5	HW11-6	839	5	NA	4	4.54	20.19	3.65	16.26
PVC	18	6	HP09-2	1376	1281	1312	2	NA			
PVC	18	6	HP09-3	1522	1470	1492	2	NA			
PVC	18	6	HP09-4	210	34	167	3	6.75	30.02	5.42	24.12
PVC	34	5	AP01-2	1479	978	1244	2	7.84	34.88	4.12	18.34
PVC	35	6	AA10-3	136	43	98	3	5.86	26.09	4.10	18.22
PVC	35	6	AP01-1	990	833	970	3	7.84	34.88	4.12	18.34
PVC	35	6	AP02-1	2382	1932	NA	5	8.96	39.86	4.10	18.22
PVC	36	6	HP02-2	185	107	128	2	6.91	30.75	4.12	18.34
PVC	36	6	HP02-3	663	220	NA	3	4.12	18.34	2.26	10.06
PVC	36	6	HA17-1	108	14	20	2	6.91	30.75	2.26	10.06
PVC	37	6	HA17-2	1808	1	29	2	6.91	30.75	3.19	14.20
PVC	37	6	AA11-3	188	35	59	3	6.91	30.75	3.19	14.20
PVC	38	7	HA13-4	1928	1896	1917	2	7.63	33.96	5.42	24.12
PVC	38	7	HP01-3	1228	883	NA	4	7.63	33.96	1.00	4.46

POLY	B#	#D	PLATE	TOTAL	I.C.	F.C.	T	MX. lb	MX. N	MN. lb	MX. N
LPE	23	3	AW08-5	1200	5	5	1	8.77	39.02	1.33	5.93
LPE	23	3	AA09-3	62	2	4	3	3.19	16.20	1.33	5.93
LPE	23	3	AW08-2	2402	NA	NA	6	7.84	34.88	2.26	10.06
LPE	23	3	AP04-1	122	14	15	1	7.84	34.88	1.33	5.93
LPE	24	4	AP03-1	116	55	56	3	7.19	31.99	2.77	12.32
LPE	24	4	AW09-5	1199	NA	NA	6	4.54	20.19	3.65	16.26
LPE	25	3	AP04-2	4807	60	90	2	6.91	30.75	1.33	5.93
LPE	25	3	AW08-4	60	0	29	4	6.91	30.76	1.33	5.93
LPE	26	3	AA08-3	62	10	11	1	3.21	14.29	1.00	4.46
LPE	26	3	AP03-2	4800	NA	NA	6	7.63	33.96	3.21	14.29
LPE	26	3	AW09-2	2539	5	5	1	11.61	51.66	2.33	10.36
LPE	26	3	AW09-4	60	9	9	1	6.31	28.06	2.33	10.36
LPE	26	3	HA17-3	76	14	15	1	5.05	22.47	4.12	18.34
LPE	26	3	HP02-5	2870	NA	NA	6	8.07	35.92	1.00	4.46
LPE	27	2	HP03-1	240	2	2	1	7.84	34.88	1.33	5.93
LPE	30	4	HW17-5	134	22	36	2	5.98	26.61	1.33	5.93
LPE	30	4	HA13-5	80	29	65	2	2.26	10.06	2.26	10.06
LPE	31	3	HP03-2	199	17	17	1	5.98	26.61	2.26	10.06
LPE	31	3	HP09-5	2727	58	1913	4	8.07	35.92	2.33	10.36
LPE	31	3	HW18-2	135	112	115	2	3.65	16.26	2.77	12.32
PSF	13	5	AW07-3	584	432	560	3	7.84	34.88	6.91	30.75
PSF	40	5	HW11-3	538	393	474	5	7.84	34.88	6.91	30.75
PSF	40	5	HW11-4	3048	1132	NA	4	7.19	31.99	4.10	18.22
PSF	40	5	AW10-2	2421	NA	NA	6	4.10	18.22	3.65	16.26
PSF	40	5	HA13-1	1497	988	NA	5	8.52	37.89	7.63	33.96
PSF	40	5	AA10-1	1301	6	NA	5	9.70	43.15	5.05	22.47
PSF	42	5	AA11-1	1788	NA	NA	6	8.96	39.86	3.21	14.29
PSF	42	5	HP01-4	83	24	36	2	7.19	31.99	4.98	22.16
PSF	42	5	AW11-2	4803	NA	NA	6	8.96	39.86	6.31	28.06
PSF	42	5	HW13-2	3590	NA	NA	6	9.40	41.82	7.63	33.96
PSF	42	5	HA11-1	301	91	115	3	7.84	34.88	4.12	18.34
PSF	42	5	HA11-2	1201	NA	NA	6	9.70	43.15	6.91	30.75
PSF	43	5	HP02-4	92	61	68	2	6.91	30.75	4.12	18.34

POLY	B#	#D	PLATE	TOTAL	I.C.	F.C.	T	MX. lb	MX. N	MN. lb	MN. N
PTF	11	5	HP09-1	2400	NA	NA	6	7.63	33.96	0.56	2.49
PTF	16	3	HP10-1	2410	1027	2115	5	5.05	22.47	1.33	5.93
PTF	16	3	AW08-1	63	8	15	2	3.66	16.27	0.40	1.79
PTF	16	3	AP03-3	898	NA	NA	6	7.19	31.99	1.00	4.46
PTF	16	3	AP03-4	4851	NA	NA	6	8.77	39.02	1.33	5.93
PTF	16	3	HW06-2	251	25	236	3	5.66	25.18	1.53	6.83
PTF	16	3	HW06-3	611	4	NA	5	5.86	26.09	0.56	2.49
PTF	16	3	AP04-4	2317	1477	NA	5	8.96	39.86	1.00	4.46
PTF	17	3	AP04-5	2401	NA	NA	6	8.07	35.92	1.00	4.46
PTF	17	3	AP04-3	1144	304	1056	5	7.84	34.88	1.33	5.93
PTF	17	3	AW09-2	42	2	4	1	5.86	26.09	0.56	2.49
PTF	20	1	AW07-2	248	2	2	1	10.73	47.72	1.44	6.42
PTF	44	5	HA17-4	410	62	406	5	6.31	28.06	0.56	2.49
PTF	44	5	AA08-6	145	21	130	3	2.33	10.36	0.56	2.49
PTF	45	5	HA18-1	235	31	NA	5	1.33	5.93	1.33	5.93
PTF	45	5	AA09-6	135	56	92	2	1.80	8.00	1.33	5.93

APPENDIX B

STATISTICAL ANALYSIS OF THIN POLYMER FILM RESEARCH DATA.

DEPENDENT VARIABLES: MIN AND MAX FRICTION

INDEPENDENT VARIABLES: POLYMER, SURFACE, AND HARDNESS

Note: The data is presented here in two types of tables. The first are tables of friction forces for the independent variables. The second are ANOVA tables for the dependent variables. ANOVA stands for analysis of variance. ANOVA tables are used here to help determine whether the mean values of a given dependent variable are equal when the data is grouped according to an independent variable.

When the means are not significantly different, the F value given in the ANOVA table will be close to 1.0. The probability of an F value greater than the observed (PR > F) will also be great. When at least one of the means is different, the F value will be greater than 1.0 and the PR > F will be small (typically .05 or less). See reference 33 for more detailed explanations of these topics.

All the mean minimum friction forces were found to be different when the independent variable was polymer film type. Therefore, the rest of the statistical tests were performed within each polymer type.

The friction force data has units of newtons. The normal load for all the experiments was 45 N.

TABLE B1. MIN AND MAX FRICTION FORCE FOR DIFFERENT POLYMERS

VARIABLE	N	MEAN	STANDARD DEVIATION	MINIMUM VALUE	MAXIMUM VALUE
POLYMER=PTFE					
MIN	16	4.4	1.8	1.8	6.8
MAX	16	27.0	12.0	5.9	47.7
POLYMER=LDPE					
MIN	20	9.3	4.0	4.5	18.3
MAX	20	28.8	10.0	10.1	51.7
POLYMER=PVC					
MIN	17	16.2	5.0	4.5	24.1
MAX	17	30.3	6.2	18.3	39.9
POLYMER=PSF					
MIN	13	24.5	7.1	14.3	34.0
MAX	13	35.6	6.8	18.2	43.2

ANOVA TABLE FOR THE DEPENDENT VARIABLE MIN FRICTION

SOURCE	DF	SUM OF SQUARES	MEAN SQUARE	F VALUE
MODEL	3	3350	1120	51
ERROR	62	1350	21.8	PR > F
TOTAL	65	4700		0.0001

R-SQUARE	C.V.	ROOT MSE	MIN MEAN
0.712	36.3	4.67	12.9

ANOVA TABLE FOR THE DEPENDENT VARIABLE MAX FRICTION

SOURCE	DF	SUM OF SQUARES	MEAN SQUARE	F VALUE
MODEL	3	590	197	2.33
ERROR	62	5230	84.4	PR > F
TOTAL	65	5820		0.082

R-SQUARE	C.V.	ROOT MSE	MAX MEAN
0.101	30.5	9.2	30.1

TABLE B2. MIN FRICTION FORCE FOR PTFE ON HARD (1) AND SOFT (2) PLATES

VARIABLE	N	MEAN	STANDARD DEVIATION	MINIMUM VALUE	MAXIMUM VALUE
HARDNESS=1					
MIN	6	4.4	2.1	2.5	6.8
HARDNESS=2					
MIN	10	4.4	1.7	1.8	6.4

ANOVA TABLE FOR THE DEPENDENT VARIABLE MIN FRICTION

SOURCE	DF	SUM OF SQUARES	MEAN SQUARE	F VALUE
MODEL	1	0.02	0.02	0.01
ERROR	14	46.7	3.3	PR > F
TOTAL	15	46.7		0.93

R-SQUARE	C.V.	ROOT MSE	MIN MEAN
0.0004	41.5	1.8	4.4

TABLE B3. MIN FRICTION FORCE FOR LDPE ON HARD (1) AND SOFT (2) PLATES

VARIABLE	N	MEAN	STANDARD DEVIATION	MINIMUM VALUE	MAXIMUM VALUE
HARDNESS=1					
MIN	8	9.7	4.4	4.5	18.3
HARDNESS=2					
MIN	12	9.0	3.9	4.5	6.3

ANOVA TABLE FOR THE DEPENDENT VARIABLE MIN FRICTION

SOURCE	DF	SUM OF SQUARES	MEAN SQUARE	F VALUE
MODEL	1	2.4	2.4	0.14
ERROR	18	302.3	16.8	PR > F
TOTAL	19	304.7		0.71

R-SQUARE	C.V.	ROOT MSE	MIN MEAN
0.0078	44.2	4.1	9.3

TABLE B4. MIN FRICTION FORCE FOR PVC ON HARD (1) AND SOFT (2) PLATES.

VARIABLE	N	MEAN	STANDARD DEVIATION	MINIMUM VALUE	MAXIMUM VALUE
HARDNESS=1					
MIN	12	15.7	5.8	4.5	24.1
HARDNESS=2					
MIN	4	17.3	2.1	14.2	18.3

ANOVA TABLE FOR THE DEPENDENT VARIABLE MIN FRICTION

SOURCE	DF	SUM OF SQUARES	MEAN SQUARE	F VALUE
MODEL	1	7.3	7.3	0.27
ERROR	14	385.5	27.5	PR > F
TOTAL	15	392.8		0.61

R-SQUARE	C.V.	ROOT MSE	MIN MEAN
0.019	32.6	5.2	16.1

TABLE B5. MIN FRICTION FORCE FOR PSF ON HARD (1) AND SOFT (2) PLATES

VARIABLE	N	MEAN	STANDARD DEVIATION	MINIMUM VALUE	MAXIMUM VALUE
HARDNESS=1					
MIN	8	25.8	7.2	18.2	34.0
HARDNESS=2					
MIN	5	22.4	7.2	14.3	30.8

ANOVA TABLE FOR THE DEPENDENT VARIABLE MIN FRICTION

SOURCE	DF	SUM OF SQUARES	MEAN SQUARE	F VALUE
MODEL	1	36.5	36.5	0.71
ERROR	11	569.4	51.8	PR > F
TOTAL	12	605.9		0.42

R-SQUARE	C.V.	ROOT MSE	MIN MEAN
0.060	29.4	7.2	24.5

TABLE B6. MIN FRICTION FORCE FOR PTFE ON GROUND AND POLISHED PLATES

VARIABLE	N	MEAN	STANDARD DEVIATION	MINIMUM VALUE	MAXIMUM VALUE
GROUND SURFACE					
MIN	9	4.1	2.1	1.8	6.8
POLISHED SURFACE					
MIN	7	4.8	1.3	2.5	5.9

ANOVA TABLE FOR THE DEPENDENT VARIABLE MIN FRICTION

SOURCE	DF	SUM OF SQUARES	MEAN SQUARE	F VALUE
MODEL	1	2.0	2.0	0.63
ERROR	14	44.8	3.2	PR > F
TOTAL	15	46.8		0.44

R-SQUARE	C.V.	ROOT MSE	MIN MEAN
0.042	40.6	1.8	4.4

TABLE B7. MIN FRICTION FORCE FOR LDPE ON GROUND AND POLISHED PLATES

VARIABLE	N	MEAN	STANDARD DEVIATION	MINIMUM VALUE	MAXIMUM VALUE
GROUND SURFACE					
MIN	12	9.7	4.4	4.5	18.3
POLISHED SURFACE					
MIN	8	8.7	3.6	4.5	14.3

ANOVA TABLE FOR THE DEPENDENT VARIABLE MIN FRICTION

SOURCE	DF	SUM OF SQUARES	MEAN SQUARE	F VALUE
MODEL	1	4.8	4.8	0.29
ERROR	18	299.9	16.7	PR > F
TOTAL	19	304.7		0.60

R-SQUARE	C.V.	ROOT MSE	MIN MEAN
0.016	44.1	4.1	9.3

TABLE B8. MIN FRICTION FORCE FOR PVC ON GROUND AND POLISHED PLATES

VARIABLE	N	MEAN	STANDARD DEVIATION	MINIMUM VALUE	MAXIMUM VALUE
GROUND SURFACE					
MIN	8	16.4	4.3	10.1	24.1
POLISHED SURFACE					
MIN	9	16.0	5.7	4.5	24.1

ANOVA TABLE FOR THE DEPENDENT VARIABLE MIN FRICTION

SOURCE	DF	SUM OF SQUARES	MEAN SQUARE	F VALUE
MODEL	1	0.6	0.6	0.02
ERROR	15	396.4	26.4	PR > F
TOTAL	16	397.0		0.88

R-SQUARE	C.V.	ROOT MSE	MIN MEAN
0.0016	31.6	5.1	16.2

TABLE B9. MIN FRICTION FORCE FOR PSF ON GROUND AND POLISHED PLATES

VARIABLE	N	MEAN	STANDARD DEVIATION	MINIMUM VALUE	MAXIMUM VALUE
GROUND SURFACE					
MIN	11	25.3	7.5	14.3	34.0
POLISHED SURFACE					
MIN	2	20.3	2.7	18.3	22.2

ANOVA TABLE FOR THE DEPENDENT VARIABLE MIN FRICTION

SOURCE	DF	SUM OF SQUARES	MEAN SQUARE	F VALUE
MODEL	1	42.4	42.4	0.83
ERROR	11	563.5	51.2	PR > F
TOTAL	12	605.9		0.38

R-SQUARE	C.V.	ROOT MSE	MIN MEAN
0.069	29.2	7.1	24.5

APPENDIX C

FILM THICKNESS CALCULATIONS USING PROJECTED IMAGE MEASUREMENTS.

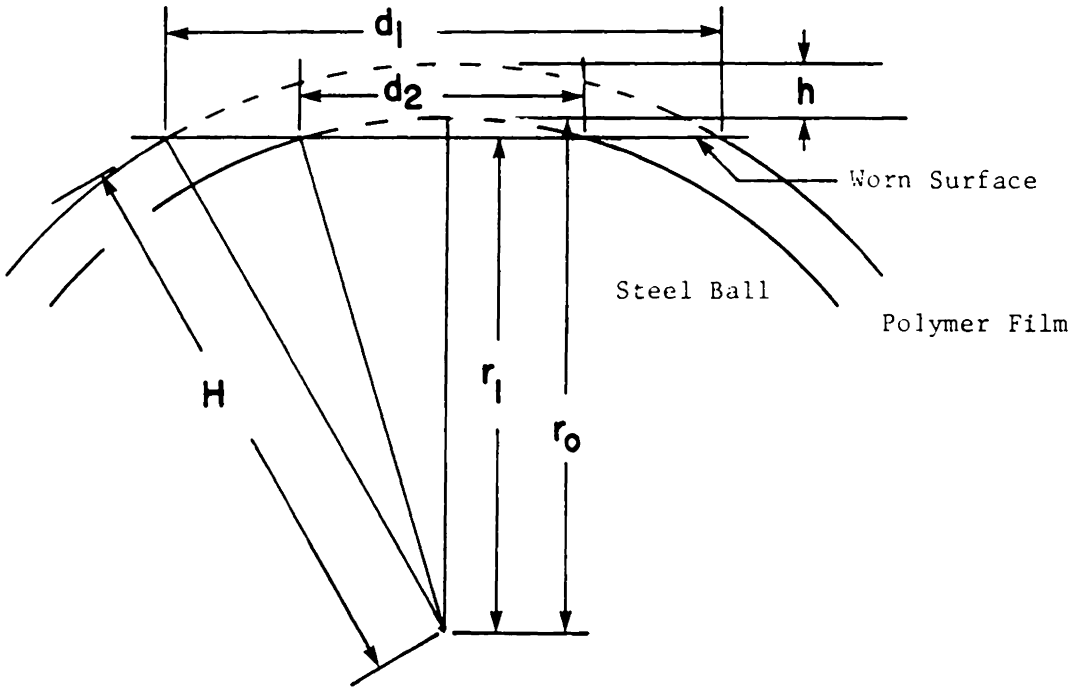

D_1, D_2 = measurements from projected image

I = image projection factor

$$H = r_o + h$$

$$H^2 = r_1^2 + \frac{d_1^2}{4} = (r_o + h)^2 = r_o + 2r_o h + h^2$$

$$h^2 + 2r_o h + r_o^2 - r_1^2 - \frac{d_1^2}{4} = 0$$

$$r_o^2 = r_1^2 + \frac{d_2^2}{4}$$

$$\frac{d_2^2}{4} = r_o^2 - r_1^2$$

$$h^2 + 2r_o h - \left(\frac{d_1^2 - d_2^2}{4}\right) = 0$$

$$d_1 = \frac{D_1}{I} \quad , \quad d_2 = \frac{D_2}{I}$$

$$n^2 + 2r_o h - \left(\frac{D_1^2 - D_2^2}{4I^2}\right) = 0$$

$$h = \sqrt{r_o^2 + \left(\frac{D_1^2 - D_2^2}{4I^2}\right)} - r_o$$

DATA FOR POLYMER FILM THICKNESS (h) CALCULATIONS.

POLY	B#	#D	PLATE	SLIDE	MAG	I	D1 in.	D2 in.	h m in.	h μm
PVC	14	5	HW13-3	Q-15	12.5X	127	9.1	1.8	1.20	30.5
PVC	36	6	HA17-1	S-10	12.5X	127	8.5	2.1	1.68	42.7
PVC	37	6	HA17-2	S-13	12.5X	127	8.6	1.7	1.76	44.7
PVC	38	7	HA13-4	S-15	12.5X	127	7.9	1.9	1.46	37.1
LPE	26	3	HA17-3	T-06	12.5X	127	9.4	2.0	2.08	77.1
LPE	26	3	HP02-5	U-16	12.5X	127	10.5	7.5	1.34	34.0
LPE	27	2	HP03-1	U-15	16.0X	163	8.5	4.7	0.76	25.9
LPE	30	4	HW17-5	T-17	12.5X	127	8.2	2.5	1.51	39.1
LPE	30	4	HA13-5	T-05	12.5X	127	8.1	0.9	1.60	40.6
LPE	31	3	HP03-2	U-18	12.5X	127	9.6	3.2	2.03	51.6
LPE	31	3	HW18-2	T-19	12.5X	127	9.8	1.5	2.32	58.9
PSF	40	5	HW11-3	Q-12	16.0X	163	9.0	0.8	1.22	31.0
PSF	40	5	HW11-4	Q-13	12.5X	127	9.1	2.8	1.85	47.0
PSF	42	5	HW13-2	Q-14	12.5X	127	9.1	2.7	1.87	47.5
PSF	42	5	HA11-1	R-07	12.5X	127	8.1	2.0	1.52	38.6
PTF	44	5	HA17-4	T-13	16.0X	163	9.1	3.6	1.06	26.9
PTF	44	5	AA08-6	U-03	12.5X	127	7.3	2.0	1.22	31.0
PTF	45	5	AA09-6	U-04	12.5X	127	7.9	3.8	1.19	30.2

Note: D1 and D2 where measured to the nearest .1 in. The film thickness was determined using these numbers. The h in um was calculated using a metric conversion factor.

The vita has been removed from the scanned document

THE EFFECTS OF THIN POLYMERIC SURFACE FILMS ON FRETTING CORROSION

by

Karl A. Sweitzer

(ABSTRACT)

The main purpose of this research is to determine if polymer films can prevent fretting between two metals, and if they can, what the protection mechanisms are. This research is a part of fretting corrosion studies currently funded by the Army Research Office. Four thermoplastic polymers were tested for their effectiveness. Two other independent variables were also tested: plate hardness and plate roughness. A ball-on-plate device was built to approximate point sliding at the fretting corrosion interface. The tribometer has two experimental positions that are electrically insulated from the rest of the apparatus so that an electrical circuit could be used to monitor metal-to-metal contact. All experiments were run with 52100 steel balls, 1040 steel plates, a normal load of 45 N (10 lbf), an amplitude of .33 mm (.013 in.) and a frequency of 20 Hz. PVC films were found to prevent fretting and metallic contact for 40 minutes. An electrochemical fretting corrosion mechanism has been suggested to explain this behavior. PTFE, LDPE, and PSF films could all produce fretting corrosion while preventing metal-to-metal contact for 40 minutes. Plate hardness and plate roughness had no statistical significance on the measured minimum fretting friction force.